HHS Public Access

Author manuscript

*Cell Rep*. Author manuscript; available in PMC 2025 January 23.

Published in final edited form as:

*Cell Rep*. 2024 November 26; 43(11): 114954. doi:10.1016/j.celrep.2024.114954.

# Netrin1 patterns the dorsal spinal cord through modulation of Bmp signaling

**Sandy Alvarez**[1,2], **Sandeep Gupta**[1], **Yesica Mercado-Ayon**[1,2], **Kaitlyn Honeychurch**[1], **Cristian Rodriguez**[1,3], **Riki Kawaguchi**[4], **Samantha J. Butler**[1,5,6,7,*]

[1]Department of Neurobiology, David Geffen School of Medicine, University of California, Los Angeles, Los Angeles, CA 90095, USA

[2]Molecular Biology Interdepartmental Graduate Program, University of California, Los Angeles, Los Angeles, CA 90095, USA

[3]CIRM Bridges to Research Program, California State University, Northridge, CA 91330, USA

[4]Department of Psychiatry, David Geffen School of Medicine, University of California, Los Angeles, Los Angeles, CA 90095, USA

[5]Eli and Edythe Broad Center of Regenerative Medicine and Stem Cell Research, University of California, Los Angeles, Los Angeles, CA 90095, USA

[6]Intellectual & Developmental Disabilities Research Center, University of California, Los Angeles, Los Angeles, CA 90095, USA

[7]Lead contact

## SUMMARY

We have identified an unexpected role for netrin1, a canonical axonal guidance cue, as a suppressor of bone morphogenetic protein (Bmp) signaling in the developing dorsal spinal cord. Using a combination of gain- and loss-of-function approaches in chicken and mouse embryonic models, as well as mouse embryonic stem cells (mESCs), we have observed that manipulating the level of netrin1 specifically alters the patterning of the Bmp-dependent dorsal interneurons (dIs), dI1–dI3. Altered netrin1 levels also change Bmp signaling activity, as assessed using bioinformatic approaches, as well as monitoring phosophoSmad1/5/8 activation, the canonical intermediate of Bmp signaling, and Id levels, a known Bmp target. Together, these studies support the hypothesis that netrin1 acts from the intermediate spinal cord to regionally confine Bmp signaling to the



*Correspondence: butlersj@ucla.edu.

AUTHOR CONTRIBUTIONS

S.A. and S.J.B. conceived the project. S.A. and K.H. analyzed the distribution of netrin1 and netrin2. S.A. and Y.M.-A. performed the chicken gain-of-function analyses, while S.A., Y.M.-A., C.R., and S.G. performed the mouse loss-of-function analyses. S.A. assessed the Bmp/netrin1 interaction *in vitro*. S.G. performed the cellular differentiations and conducted bulk RNA-seq. S.G. and R.K. analyzed the bulk RNA-seq data. This paper was written by S.A., S.G., and S.J.B. and edited by S.A., S.G., and S.J.B.

DECLARATION OF INTERESTS

The authors declare no competing interests.

SUPPLEMENTAL INFORMATION

Supplemental information can be found online at https://doi.org/10.1016/j.celrep.2024.114954.

dorsal spinal cord. Thus, netrin1 has reiterative activities shaping dorsal spinal circuits, first by regulating cell fate decisions and then acting as a guidance cue to direct axon extension.

## In brief

Alvarez et al. use loss- and gain-of-function approaches in chicken, mouse, and stem cells to show that netrin1 inhibits Bmp activity to confine dorsal neural patterning to the correct compartment in the embryonic spinal cord. Netrin1 regulates mRNA processing to suppress Bmp signaling.

## Graphical Abstract

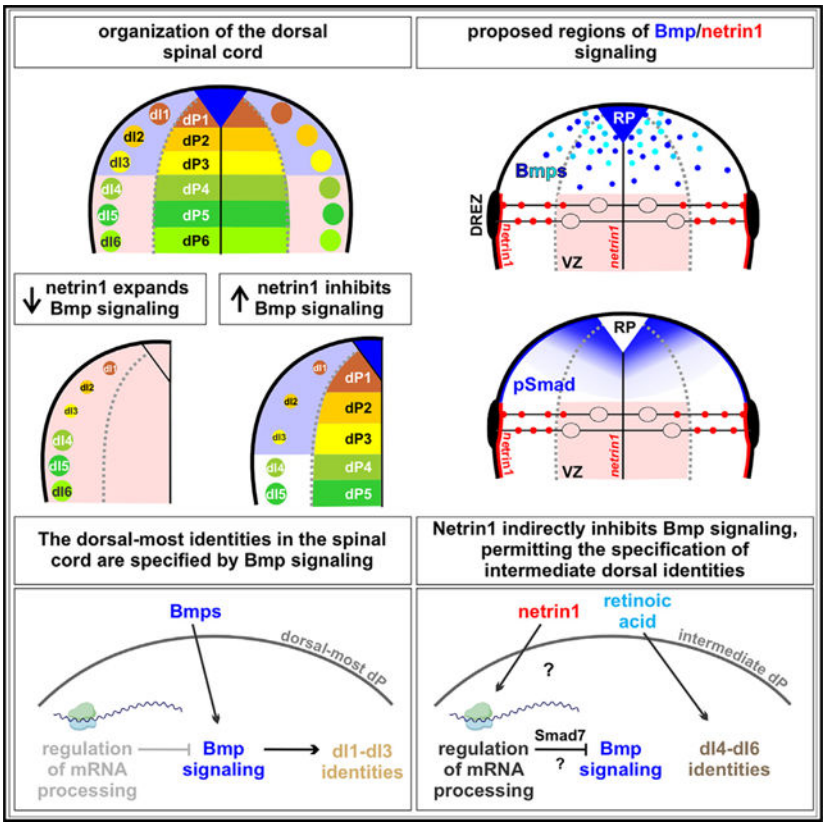


## INTRODUCTION

Netrin1 is a laminin-like protein that was first characterized for its axon guidance activities during embryonic development.[1,2] Netrin1 is widely expressed in both the developing and adult nervous systems, including in the forebrain, optic disc, cerebellum, and spinal cord,[1,3–5] as well as in various tissues outside of the nervous system, including the lung, pancreas, mammary glands, intestine, and developing heart.[6–10]

Many studies have focused on the role of netrin1 directing neural circuit formation in the developing spinal cord, where it was initially identified.[1,2] Spinal neurons arise at stereotyped positions along the dorsal-ventral axis, such that the dorsal spinal cord is composed of at least six populations of dorsal interneurons (dIs), dI1–dI6, which are

derived from six dorsal progenitor (dP) domains, dP1–dP6.[11,12] This pattern is generated by multiple signals, which collectively act on proliferating neural progenitor cells (NPCs) in the ventricular zone (VZ).[11,12] In the dorsal spinal cord, these signals include multiple members of the bone morphogenetic protein (Bmp) family, which are secreted from the roof plate (RP) at the dorsal midline of the spinal cord.[13,14] Bmps are sufficient for the specification of the RP itself, as well as the dI1s, dI2s, and dI3s.[15–19] The Bmps activate distinct type I Bmp receptors,[18,20] which in turn phosphorylate the receptor-regulated (R)-Smads, Smad1/5/8, the intracellular mediators of Bmp signaling,[21] to direct dPs to differentiate into post-mitotic dIs.[22] Bmps have reiterative roles, directing both NPC proliferation and dI differentiation.[18] Additional signals include retinoic acid (RA), which is present in the surrounding paraxial mesoderm and is important for patterning and neuralization.[23–25] Immediately after neurogenesis, dIs start to extend axons toward their synaptic targets.[26] Netrin1 acts to direct dI1 and other commissural axons toward the floor plate (FP), at the ventral midline of the spinal cord.[1] While *netrin1* is expressed by both NPCs in the intermediate VZ, and the FP in the mouse spinal cord, recent studies have suggested that it is the NPC-derived netrin1 that is most critical for mediating axon guidance events.[27–30] NPC-derived netrin1 is thought to be trafficked along the radial processes of the NPCs until it is deposited on the pial surface, where it forms an adhesive growth substrate that locally orients commissural axon extension.[28–30]

The netrin family has subsequently been shown to play many critical roles in developmental and physiological processes beyond axon guidance. Netrin1 is involved in the progression of cancers,[31–35] diabetes,[36] and inflammatory bowel diseases.[37] Netrin1 also directs cellular differentiation across organ systems. In the skeletal system, netrin1 mediates bone remodeling by suppressing osteoclast differentiation and promoting osteoblast differentiation.[38] Netrin1 also plays a role in the morphogenesis and differentiation of the mouse mammary glands[39] and can induce human embryonal carcinoma cells to differentiate into a neuroectodermal-like cell type.[40] However, no role for netrin1 directing cell fate in the developing nervous system *in vivo* has been described.

Here, we provide evidence that netrin1 can regulate cell fate specification in the dorsal spinal cord. Since netrin1 has been previously shown to suppress the Bmp signaling pathway in different cell types *in vitro*,[41] we sought to investigate the relationship between netrin1 and Bmp signaling in the patterning of the embryonic spinal cord. These studies support the hypothesis that netrin1 acts from the intermediate spinal cord to regionally limit the extent of Bmp signaling to the dorsal spinal cord. Using a combination of bioinformatics with gain- and loss-of-function approaches in chicken, mouse, and stem cell models, we have found that modulating the level of netrin1 has profound effects on the number of the Bmp-dependent dIs (i.e., dI1–dI3). Netrin1 appears to mediate its effects through the Bmp pathway, given that changes in dI number were accompanied by alterations in the levels of both phosopho (p) Smad1/5/8 and inhibitor of differentiation/DNA-binding (Id) expression. The Id family are key downstream mediators of Bmp signaling[42] that modulate the activities of the proneural basic-helix-loop-helix (bHLH) proteins[43–45] to prevent exit from the cell cycle.[46,47] Thus, activation of Ids can result in NPCs being held in a proliferative state.

Together, these findings suggest an unexpected role for netrin1 in the developing spinal cord, modulating Bmp signaling to fine-tune neural patterning. Thus, netrin1 has an earlier role than previously realized, with reiterative activities shaping dorsal spinal circuits, first by regulating cell fate decisions and then acting as a guidance cue to direct axon extension. Both netrin1 and members of the Bmp family are widely expressed, with the Bmps also having reiterative roles in cell growth, differentiation, migration, apoptosis, and homeostasis in the developing embryo and adult.[48–50] These studies therefore also open the possibility that netrin1 can modulate Bmp-dependent processes in other organs.

## RESULTS

### Netrin family expression in the developing spinal cord

Netrin1 has widespread expression in the developing mouse spinal cord; it is expressed by cells in the FP and the ventral and intermediate NPCs, resulting in netrin1 protein decorating the ventral and intermediate pial surface.[29,30] In contrast, netrin function is mediated by both netrin1 and netrin2 in the embryonic chicken spinal cord, which have distinct distributions at different stages (Figures 1A–1L).[1,51] At Hamburger Hamilton (HH) stage 18, when dI fate specification commences,[18] netrin1 is present in the ventral spinal cord (Figures 1A and 1B), while netrin2 is present in the intermediate spinal cord, and is absent from the dorsal- and ventral-most regions (arrowheads, Figure 1F). By HH stage 24, when axonogenesis is ongoing, *netrin1* expression is confined to the FP (arrowhead, Figure 1I), while the domain of netrin2 has contracted to an intermediate region that spans from immediately below the dorsal root entry zone to just above the motor column (arrowheads, Figures 1K and 1L). In both cases, the distribution of *netrin* mRNA is largely distinct from the distribution of netrin protein. This is most evident for netrin2: *netrin2* mRNA is present in the VZ, while netrin2 protein accumulates on the pial surface immediately adjacent to its expression domain. Thus, the expression patterns of chicken netrin1 and netrin2 are the composite of the mouse netrin1 distribution, including the conserved upper boundary in the dorsal spinal cord.

### Netrin1 misexpression does not perturb the architecture of the spinal cord

To investigate whether netrin1 has effects in the spinal cord distinct from its role mediating axon guidance, we first assessed whether the misexpression of netrin1 altered the general structure of the chicken spinal cord. A range of concentrations (50 ng, 500 ng, and 1 μg) of C-terminally myc-tagged netrin1 DNA plasmid (netrin1-myc) were electroporated into the HH stage 14 spinal cord under the control of the ubiquitously expressed CAG enhancer,[52] and the consequences examined 2 days later, at HH stage 24/25. CAG::*gfp* was concomitantly electroporated in all experiments, to both serve as a control (Figures 1M–1R) and indicate the extent of electroporation. Initially, both chicken and mouse netrin1 were used in these experiments, which are ~90% similar at the amino acid level. However, since their activities were found to be very similar (data not shown), we proceeded with mouse netrin1, which could be additionally identified as a distinct signal using species-specific antibodies. While the GFP fluorophore had no effect on the distribution of endogenous chicken netrin1 (arrow, Figures 1M and 1O), the misexpression of netrin1-myc resulted in both myc and netrin1 being targeted to the pial surface (arrows, Figures 1S–1U and 1Y–1AA). Increasing the concentration of electroporated netrin1-myc increased the amount

of pial-myc (compare arrows, Figures 1T and 1Z). However, even at the highest levels of exogenous netrin1-myc, there was no effect on the integrity of the laminin$^{+}$ basal membrane (Figures 1V, 1W, 1BB, and 1CC) or the nestin1$^{+}$ radial processes of the NPCs (Figures 1X and 1DD) compared to control electroporations (Figures 1P–1R). Thus, misexpression of netrin1 does not change the overall architecture of the spinal cord.

## Netrin1 overexpression in chicken embryos results in a dose-dependent reduction in dIs

Although the general architecture of the spinal cord was unaffected, we did observe a reduction in the size of the spinal cord after electroporation with netrin1-myc. To further assess this phenotype, we quantified the area bounded by either the Sox2$^{+}$ NPCs or p27$^{+}$ post-mitotic neurons in control (Figures 2A–2C and 2N) versus netrin1-myc (Figures 2D–2F and 2N) electroporations. In the control condition, the electroporated vs. non-electroporated sides of the embryo were statistically indistinguishable for both Sox2$^{+}$ NPCs ($p > 0.65$, Student's t test) or p27$^{+}$ neurons ($p > 0.60$). In contrast, there was a ~25% reduction in the total area bounded by Sox2$^{+}$ NPCs and ~33% decrease in area of the p27$^{+}$ neurons after ectopic expression of netrin1-myc (Figure 2N). This reduction was seen with all concentrations of netrin1, suggesting that netrin1 can potently affect the number of neurons that arise in the spinal cord.

While the size of the entire spinal cord was reduced, the effect of netrin1 on the dorsal spinal cord was more pronounced and observed even at the lowest concentrations (Figure 2O). To further assess the consequence of netrin1 misexpression on specific dorsal identities, we used a well-described panel of antibodies against transcription factors that distinguish specific dI fates[53] to monitor the numbers of Lhx2$^{+}$ dI1s, Lhx1/5$^{+}$ Pax2$^{-}$ dI2s, Isl1$^{+}$ dI3, and Lhx1/5$^{+}$ Pax2$^{+}$ dI4s. We observed that the Bmp-dependent populations,[25] i.e., dI1, dI2, and dI3, are all significantly reduced after netrin1-myc electroporation compared to the GFP control. These reductions were concentration dependent, such that more dI1/dI2/dI3s were lost as the amount of netrin1-myc increased. ~75% of dI1s and ~50% of dI2/dI3s were ablated at the highest concentration of netrin1-myc tested (Figure 2R). We also observed the profound loss of dI1 commissural axons from the remaining dI1 population (Figure S2).

In contrast, the dI4s, a Bmp-independent population, were less profoundly affected. The lowest level of netrin1-myc did not significantly affect the numbers of dI4s; rather, dI4s were only lost as the concentration of netrin1-myc increased (Figure 2R). The more widespread loss of neurons resulting from the highest levels of netrin1-myc misexpression appears to be a consequence of cell death. The number of caspase$^{+}$ cells was not significantly different between control and 50-ng CAG:: *netrin1-myc*, but it did increase as the concentration of netrin1-myc increased (Figure 2Q).

## Addition of netrin1 to mESCs blocks their ability to acquire dI1/dI3 fates

We next assessed the activity of netrin1 in a stem cell model that recapitulates the early events that direct cell fate in the developing spinal cord.[25] In brief, bFGF/Wnt signaling directs mouse embryonic stem cells[54] (mESCs) into a bipotential neuromesodermal progenitor (NMP) fate, which is a critical intermediate for the cells of the caudal neural tube[55] (Figure 3A). Our recent work has shown that addition of RA, from day 3–5 directs

NMPs to a caudal dorsal progenitor (dP) fate, specifically that of the intermediate neural tube, ultimately resulting in the specification of dI4, dI5, and dI6.[25,56] The sequential addition of Bmp4 from day 4–5 further dorsalizes the NMPs into the dPs that specify the dI1, dI2, and dI3 fates. Thus, these RA ± Bmp4-directed differentiation protocols provide an additional model to investigate the mechanisms that drive dorsal spinal cord development.

Using genomic data from our prior studies[25,57] we determined that *netrin1* is expressed by mESC-derived progenitors but is generally absent from differentiating neurons (Figure S1A), as *in vivo*.[2,30] We assessed the effect of adding two concentrations of exogenous netrin1−0.125 μg/mL (low) and 0.5 μg/mL (high)− to mESC-derived NMPs in the RA ± Bmp4 protocols at three different time points. Netrin1 was added concomitantly with Bmp4 from day 4–5 (condition 1); immediately after Bmp4 treatment from day 5–6 (condition 2); and finally, for an extended period after Bmp4 treatment from day 5–9 (condition 3) (Figure 3A). The cultures were then assessed for the specification of the dorsal-most dIs at day 9 using qPCR analyses (Figures 3B–3D). The addition of netrin1 with, or immediately after, Bmp4 treatment had no apparent effect on the identity of the cultures (Figures 3B and 3C). We also found no effect on *Foxd3* expression in any of the conditions; i.e., dI2s continue to assume their fate in the presence of netrin1. However, prolonged treatment with 0.5 μg/mL netrin1 in the RA + Bmp4 protocol significantly reduced the expression of *Lhx2* and *Lhx9*, both markers of dI1s, and there is a trend ($p < 0.07$) toward the loss of *Isl1*, a dI3 marker. Thus, the extended treatment of stem cell-derived NMPs with high levels of netrin1 is sufficient to prevent some dorsalization. This result, coupled with the observation that netrin1 misexpression in the chicken spinal cord most effectively suppresses the Bmp-dependent dIs, suggests that netrin1 is sufficient to counteract the activities of the Bmps.

## The loss of netrin1 increases the size and number of the dorsal-most spinal progenitors

We next assessed the requirement for netrin signaling on dorsal spinal fate specification using mice deficient for *netrin1*.[29,58,59] We analyzed a null allele for netrin1 (*ntn1*$^{-/-}$), which was previously analyzed for axon guidance defects in the developing spinal cord[60] but was not evaluated for changes in dorsal cell fate. We focused our analysis on embryonic (E) day 11.5, when dorsal fate specification is robustly ongoing in the spinal cord. We first observed a marked expansion of the dorsal-most progenitor domains flanking the RP in the *netrin1* mutants. The dP1 domain is almost 2-fold larger in size ($p < 0.0001$, significantly different compared to littermate control) and there is a ~25% increase in the number of Atoh1$^+$ dP1s ($p < 0.045$; Figures 4A, 4D, and 4M). The dP2 domain is ~60% larger ($p < 0.0001$; Figures 4A, 4D, and 4M), as measured by the area bounded by the bottom of the Atoh1$^+$ dP1 domain and the top of Ascl1$^+$ dP3 domain. There is also a ~40% increase in the area ($p < 0.0001$) demarked by Ascl1$^+$ cells, which form the dP3–dP5 domain (Figures 4A, 4D, and 4M). In contrast, we observed no significant difference in the area of Ptf1a$^+$ ($p > 0.85$) or Olig2$^+$ ($p > 0.25$) cells in control and mutant sections (Figures 4B, 4E, 4M, and 4N), suggesting that there was no effect on either the dP4[61] or motor neuron progenitor (pMN)[62] domains. Together, these results suggest that the loss of *netrin1* increases the number/size of the most dorsal neural progenitors in the spinal cord. The increase in dPs did not stem from an increase in the rate of cell division, since there was no significant change in the number

of $pH3^+$ cells in mitosis ($p > 0.5$; Figures 4C, 4F, and 4G), or from altered patterns of cell death ($p > 0.055$; Figure 4H).

We next assessed whether the increased number of dorsal progenitors affected the number of post-mitotic dIs. To our surprise, we found that there was a ~30% decrease in the number of $Lhx2^+$ dI1s ($p < 0.0001$; Figures 4I, 4K, and 4N), $Foxd3^+$ dI2s ($p < 0.017$; Figures 4I, 4K, and 4N) and $Isl1^+$ $Tlx3^+$ dI3s ($p < 0.0001$) (Figures 4J, 4L, and 4N). In contrast, there was no significant difference in the more intermediate dIs, i.e., the $Pax2^+$ dI4s ($p > 0.67$), $Tlx3^+$ $Isl1^-$ dI5s ($p > 0.19$), and $Pax2^+$ dI6s/v0/v1 (dI6+; $p > 0.48$), or the $Isl1^+$ MNs ($p > 0.36$). Thus, the loss of netrin1 appears to specifically affect the development of the Bmp-dependent dorsal-most dIs and does not affect the Bmp-independent intermediate dIs and ventral spinal cord. This result is consistent with the hypothesis that netrin1 regulates the activity of Bmps in the dorsal spinal cord.

## Netrin1 regulates Bmp signaling in stem cell-derived dorsal progenitors

To further dissect the mechanism by which netrin1 regulates dI specification, we assessed the transcriptomic profiles of mESC-derived neural progenitors undergoing the RA + Bmp4 directed differentiation protocol in the presence of netrin1 protein (Figure 5A). Samples for bulk RNA sequencing (RNA-seq) analyses were collected on day 5 (condition 1), day 6 (condition 2), and day 9 (condition 3) (Figure 5A). Surprisingly, we observed almost no transcriptional changes between the control (RA + Bmp4 alone) and netrin1-treated samples in condition 1 (one gene down regulated, false discovery rate [FDR], $p < 0.05$). In contrast, there were a modest number of differentially expressed genes in condition 2 (26 downregulated, 19 upregulated, FDR $p < 0.05$) and a substantial number in condition 3 (4,847 downregulated, 4,125 upregulated, FDR $p < 0.05$) (Figures 5B and 5C). Thus, netrin1-mediated transcriptional changes only occur once progenitors commit to a dorsal identity.

To gain insight into the signaling pathways affected by netrin1 treatment, we conducted Gene Ontology (GO) analyses of condition 2 and 3 (Figure 5D). Supporting the hypothesis that netrin1 suppresses the Bmp signaling pathway, the Smad signal transduction gene module was downregulated at day 6 (Figure 5E). Similarly, we observed that Bmp2 target genes[63] were among the gene sets associated with previously published studies that were downregulated in condition 3. In particular, the gene network regulated by the Egr1 transcription factor was downregulated in condition 3, which includes many known transcriptional targets of Bmp signaling, such as *Id3*, *Smad7*, *Wnt4*, and *Mapk14* (Figure 5F; Table S1). Egr1 is also thought to be regulated by Bmp signaling.[64] By day 9, the upregulated GO signatures suggest that netrin1 regulates mRNA processing (Figure 5D). Many upregulated genes in condition 3 are associated with mRNA processing and splicing (Figure 5G), such *Ppig*, an RNA-binding protein,[65] and *Rnpc3*,[66] which encodes part of the spliceosome. Taken together, these transcriptomic analyses suggest a mechanism where netrin1 acts to inhibit Bmp signaling, perhaps by regulating the mRNA processing of Bmp target genes, such as the Ids, to control dI fate specification.

### The gain or loss of netrin1 activity alters the level of Bmp signaling

We next directly examined whether modulating netrin1 levels affects Bmp signaling by monitoring phosphorylated (p) Smad1/5/8 levels[67,68] in Cos7 cells *in vitro*. Cos7 cells can endogenously transduce Bmp signaling; the level of pSmad1/5/8 robustly increases when Cos7 cells are treated with Bmp4 for an hour (Figures 6H and 6K). However, if 0.5 μg/mL netrin1 is added concomitantly with Bmp4, pSmad1/5/8 levels decrease by ~60%. This is a dose-dependent response: halving the amount of netrin1 diminishes this response, while 0.125 μg/mL netrin1 treatment has no significant effect on Smad1/5/8 activation (Figures 6H and 6K).

We then assessed whether the gain or loss of netrin1 activity can alter the level of Bmp signaling *in vivo*. Bmps act from the RP at the dorsal midline to pattern the surrounding tissue.[11,12] In both chicken (Figure 6B) and mouse (open arrowheads, Figures 6A and 6F), Bmp signaling can be visualized as a graded pSmad1/5/8/signal flanking the RP.[22] The pSmad signal can also be detected on the pial surface in the dorsal-most spinal cord, extending as far as the dorsal netrin1 boundary (closed arrowheads, Figure 6A). Electroporation of mouse netrin1 into the chicken spinal cord suppresses this signal in a dose-dependent manner. Thus, there is a >50% inhibition of pSmad activation at high (1 μg) levels of netrin1 (arrows, Figures 6E and 6I), while lower (500 ng, 50 ng) levels of netrin1 suppress pSmad activation by 25% (arrows, Figures 6C, 6D, and 6I). In contrast, we observed that the area of pSmad activation is expanded by ~40% in spinal cords taken from *netrin1* mutant mice, compared to littermate controls (Figures 6F, 6G, and 6J). Thus, the level of netrin1 has an inverse effect on the activation of Bmp signaling, consistent with the model that netrin1 acts directly as a Bmp inhibitor.

### Altering netrin1 activity alters the level of Id signaling

Our bioinformatic analyses (Figure 5) implicated that netrin1 also regulates Bmp target genes. Since Id genes are well known targets of Bmp signaling, we assessed *Id1* and *Id3* expression in control (Figures 7A and 7C) and *netrin1*$^{-/-}$ (Figures 7B and 7D) mouse spinal cords. Loss of netrin1 results in ~35%–40% increase in the area of both *Id1* (bracket, Figure 7E) and *Id3* (bracket, Figure 7F) expression in the dorsal-most spinal cord. Conversely, ubiquitous expression of netrin1 in chicken spinal cords reduces *Id1* expression by ~35% (arrows, Figures 7J, 7K, and 7M). We did not observe a decrease in the intensity Id3 expression, although the staining did appear to be more diffusely distributed (arrows, Figures 7J, 7L, and 7N). Taken together, these data suggest that the loss/gain of netrin1 results in increased/decreased Bmp signaling, which in turn alters Id levels. Increased Id expression is predicted to maintain neural progenitors in an undifferentiated state, consistent with our observation that the loss of netrin1 results in more dPs at the expense of the dIs (Figure 4M, 4N, 7O, and 7P).

## DISCUSSION

Netrin1 was first shown to suppress Bmp signaling in cell lines *in vitro*.[41] Here, we have used gain and loss-of-function approaches to examine whether netrin1 modulates Bmp signaling in the developing spinal cord using a combination of *in vivo* and *in vitro* model

systems. Together, these studies suggest that netrin1 acts to limit Bmp signaling to the dorsal-most spinal cord.

Previous studies have shown that Bmp signaling directs the dI1–dI3 spinal identities (Figure 7Q)[11,12] and that the extent of Bmp signaling can be inferred from a domain of pSmad1/5/8 activity extending into the VZ.[22] Our studies support the model that a further critical difference between the dorsal-most dPs and the intermediate dPs is the presence of netrin1 (Figures 7Q and 7R). Netrin1 has an upper boundary in the intermediate dorsal spinal cord that inversely correlates with the position of the pSmad1/5/8 domain (Figure 6A). We have found that increased netrin1 levels reduces pSmad1/5/8 activity (Figure 6) and results in the preferential loss of dI1–dI3 (Figure 2). While the highest levels of netrin1 in the gain-of-function experiments appeared to generally promote cell death, we were able to identify a level of netrin1 misexpression where we observed the specific loss of dI1–dI3, with no concomitant increase in apoptosis (Figures 2Q and 2R). In contrast, we found that the loss of netrin1 function specifically expands the pSmad1/5/8 domain, apparently resulting in an increase in the number of dP1–dP3s. These dPs appear to be maintained in a progenitor state because the number of dI1s–dI3s concomitantly decrease (Figure 4N). Previous studies have shown that Bmps are reiteratively required during neurogenesis, having roles in progenitor maintenance, proliferation, and differentiation.[18,69] Here, we observed that *Id* gene expression, transcriptional targets of Bmp signaling that block differentiation, was increased in the absence of netrin1 (Figures 7A–7F). Thus, the loss of netrin1 appears to elevate Bmp signaling in a manner that drives higher levels of Id expression, which then maintains dPs in a progenitor state (Figures 7O and 7P).

Taken together, we propose that the netrin1 boundary constrains the influence of Bmp signaling to the dorsal-most region of the developing spinal cord (Figure 6L). The ability of netrin1 to modulate Bmp signaling in the spinal cord is an unexpected role for netrin1, which is best known for its role as an axon guidance cue.

### Assessing the mechanisms by which netrin1 mediates cell fate specification

The netrin1 boundary in the intermediate spinal cord is immediately adjacent to the dI1–dI3 domain (Figures 6A and 6L), suggesting that netrin1 might inhibit Bmp signaling by a direct physical interaction with Bmp ligands. Several extracellular Bmp antagonists, including gremlin and noggin, are thought to act by sequestration (i.e., as a sink to prevent Bmp ligands from binding to the Bmp receptor).[70] We found no evidence of such a direct interaction between Bmp4 and netrin1 in the directed differentiation protocols. If netrin1 acted to sequester Bmp4, then the presence of netrin1 should have inhibited Bmp4 function in all conditions tested (Figure 3A). Rather, we observed that dorsalization was only suppressed when netrin1 was added for a prolonged period to cells already in the dP state (condition 3). Netrin1 had no effect on either transcriptional activity (Figures 5B and 5C) or dorsalization when it was added concomitantly with Bmps to cells in an earlier competence state (condition 1).

These bioinformatic analyses suggested an alternative mechanistic hypothesis: that netrin1 acts through the regulation of mRNA processing to suppress Bmp signaling. Our bioinformatic analyses found that extended netrin1 treatment resulted in the upregulation of

genes associated with mRNA processing and splicing. Netrin1 was previously implicated in mRNA processing in *Aplysia*, where it was found to promote local translation of ubiquitously expressed RNAs to provide spatial control during synapse formation.[71] Thus, the presence of netrin1 may stabilize the production of Bmp inhibitors known to act in the intermediate spinal cord, such as the inhibitory Smad, Smad7.[72] When Smad7 is ectopically expressed in the developing spinal cord, the intermediate fates are expanded at the expense of the dorsal-most fates.[73] The local translation of Smad7, or other inhibitory factors, by netrin1 in the intermediate spinal cord would suppress Bmp signaling and thereby permit the specification of the intermediate dI4–dI6 fates (Figure 7R).

### Autonomy vs. non-autonomy of netrin1 signaling

A conundrum in these studies is that netrin1 is expressed in the intermediate spinal cord but results in a non-autonomous loss-of-function phenotype, expanding the size of progenitor domains in the dorsal-most spinal cord, coupled to the loss of dI1–dI3. We nonetheless hypothesize that netrin1 does function autonomously in the intermediate spinal cord to regulate cell fate. Netrin1 is a member of the laminin superfamily (i.e., an extracellular matrix component) that is thought to act at very short range to control axon guidance decisions.[28,29] Thus, it is unlikely that netrin1 acts by diffusion, such that it could directly reach, and signal to, more dorsal cells. Rather, we hypothesize that netrin1 blocks Bmp signaling in the intermediate spinal cord (Figure 7R). Removing netrin1 permits increased Bmp signaling, which results in an expansion in the size of the dorsal-most spinal cord. The dP1–dP3s adjust their boundaries in a compensatory manner, thereby resulting in larger domains (Figure 6L). The most profound effect is on the area of the domain, but we also observed an increase in the number of dPs (Figure 4M). As already discussed, this effect may result from the maintenance of the progenitor state, given that we do not observe an increase in proliferation (Figures 4C, 4F, and 4G). Since the loss of netrin1 did not affect the size of the dP4 domain (Figures 4B, 4E, 4M, and 4N), netrin1 does not appear to be directly required to specify intermediate identities. Rather, netrin1 blocks the Bmp-mediated fates to permit intermediate progenitors to adopt the alternative dP4-dP6 fates.

It also remains unresolved where netrin1 and Bmp signaling interact in the intermediate spinal cord. Our current model predicts that netrin1 acts on intermediate progenitor cells to prevent them from responding to the Bmp ligand. While there are low levels of netrin1 protein in the VZ, VZ-derived protein is present at highest levels on the pial surface[28,29] (Figure 6A). Interestingly, pSmad1/5/8 is also present on the pial surface, with an inverse distribution to that of pial-netrin1 (closed arrowheads, Figure 6A). However, the pial surface is not a cellular substrate, making it unlikely that this is the site of the netrin1/Bmp interaction. It may rather be a readout of proteins that are trafficked along the radial processes of the neural progenitors, again supporting the hypothesis that the domain of Bmp signaling is immediately adjacent to the netrin1 domain.

### Role of canonical netrin1 receptors mediating suppression of Bmp signaling

Netrin1 binds to different receptors, including Dcc, neogenin1, and members of the Unc5 family, many of which are present in the dorsal spinal cord.[29,74,75] It remains unresolved which of these receptors mediates the ability of netrin1 to regulate Bmp signaling. Our

previous studies have shown that *Dcc* is consistently expressed at low levels in the dorsal and intermediate VZ, while *neogenin1* has a more dynamic expression pattern first in the intermediate VZ and then in the dorsal-most progenitors.[75] The studies using the stem cell directed differentiation model identified a putative time window when the netrin1 cell fate receptor(s) might function. We observed that netrin1 treatment only affects the transcriptional status of stem cell-derived progenitors when added on day 5, but not at day 4 (Figures 5B and 5C). One explanation for this observation is that the receptor complement needed to respond to netrin1 is only present on day 5 (i.e., once spinal progenitors transition to the dP state). Analysis of the single-cell RNA-seq (scRNA-seq) atlas derived from the RA ± Bmp4 protocols[57] (https://samjbutler.shinyapps.io/Data_Viewer/) shows that Dcc, neogenin1, Unc5c, and Unc5d are expressed at different time points along the differentiation trajectory (Figures S1B–S1E). However, only Dcc has the profile that fits the observed netrin1 responsiveness (i.e., that the expression of Dcc is upregulated immediately after transitioning from the progenitor state).

While this analysis supports the hypothesis that Dcc is a cell fate receptor, other receptors must also be required. Dcc is not present in the chicken genome, and neogenin1 has been proposed as the functional substitute.[75] Netrin1 was able to suppress pSmad1/5/8 activity in a dose-dependent manner in Cos7 cells after Bmp4 stimulation (Figures 6G and 6K). However, we were unable to detect that either Dcc or neogenin1 are present in Cos7 cells by western analyses (data not shown). Future studies will assess whether netrin1 is interacting Dcc and/or another receptor to inhibit Bmp signaling.

## Broader implications

The Bmp family of growth factors is used to specify developmental decisions in all organ systems, in a manner that is conserved across species. While netrin1 was first studied for its axon guidance activities in the nervous system, subsequent studies have shown that it plays critical roles in the development of other organs, including the kidney, lungs, and mammary glands, as well as in the progression of diseases, such as cancer and diabetes. Thus, it is likely that the interaction between netrin1 and Bmp signaling observed in these studies will be critical for other developmental and disease processes, potentially as a fine-tuning mechanism that permits topographic regulation.

## Limitations of the study

Our studies suggest that netrin1 regulates cell fate specification by blocking Bmp signaling in the intermediate spinal cord. While this finding was consistent across multiple model systems, the implication that mRNA processing is the downstream mechanism used by netrin1 to modulate cell fate was demonstrated using an *in vitro* mESC model and has not yet been assessed *in vivo*. Additionally, it is unresolved how netrin1 regulates mRNA processing and the specific mRNAs that are putatively regulated by netrin1 to suppress Bmp signaling have not yet been identified. As discussed above, these studies also do not identify how netrin1 interacts with Bmp signaling, other than it is unlikely to be a direct interaction, and the identity of netrin1 receptor(s) that mediate the cell fate specification activities of netrin1 is unresolved. While Dcc is a leading candidate in the mouse models, Dcc is unlikely to have a role in the chicken system also tested in these studies.[75]

# RESOURCE AVAILABILITY

## Lead contact

Further information and requests for resources and reagents should be directed to Samantha Butler (butlersj@ucla.edu).

## Materials availability

Information regarding the resources and reagents used in this paper should be directed to the lead contact, Samantha Butler.

## Data and code availability

- Bulk RNA-seq data have been deposited at GEO and are publicly available. Accession numbers are listed in the key resources table. Microscopy data reported in this paper will be shared by the lead contact upon request.
- This paper did not generate custom code.
- Any additional information needed to reanalyze the data reported in this paper is available from the lead contact upon request.

# STAR★METHODS

## EXPERIMENTAL MODEL AND STUDY PARTICIPANT DETAILS

Fertile Leghorn eggs (CJ Eggs, Sylmar CA) were incubated for 60 h until the embryos reached Hamburger Hamilton stages 14–15. The spinal cord was *in ovo* electroporated as previously described[20] and allowed to develop until HH stages 24–26, at which time the tissue was analyzed.

The netrin1 null line was a gift from Dr. Lisa Goodrich.[60] Embryos were collected from timed matings, and the presence of a vaginal plug was considered embryonic day (E) 0.5. Heads were used to isolate the DNA and were amplified by PCR to identify the genotypes of each embryo.[60] All animal procedures were carried out in accordance with University of California Los Angeles IACUC guidelines.

Cos7 cells (ATCC CRL-1651) were cultured in Dulbecco's modified Eagle's medium (DMEM) (Sigma-Aldrich) supplemented with 10% fetal bovine serum (FBS) (Fisher Scientific) and Penicillin-Streptomycin-Glutamine (100X) (Gibco, Fisher Scientific).

## METHOD DETAILS

**In ovo electroporation of chicken embryos—**A c-myc tag (EQKLISEEDL) was fused to the C terminal end of mouse *netrin1* (Addgene #71978) using PCR cloning. Netrin1-myc was then subcloned into the CAGGS vector, under the control of the CAG enhancer,[78] which is comprised of a CMV enhancer and chicken β-actin promoter. Fertile Leghorn eggs (CJ Eggs, Sylmar CA) were incubated for 60 h until the embryos reached Hamburger Hamilton stages 14–15. The spinal cord was *in ovo* electroporated as previously

described[20] and allowed to develop until HH stages 24–26, at which time the tissue was analyzed.

The following constructs were used: CAG:*gfp* (1000 ng/μl), CAG:*ntn1-myc* (50 ng/μl, 500 ng/μl, or 1000 ng/μl). In all cases, the presence of GFP demonstrates electroporation efficiency. When altering the concentration of *netrin* expression the CAG:*ntn1-myc* expression vector was diluted with the pCAGEN vector (plasmid #11160, Addgene), to hold the concentration of DNA constant at 2000 ng/μl across all experiments.

**Tissue processing—**Spinal cords were fixed using 4% paraformaldehyde for 2 h at 4°C. After fixation, the tissue was cryoprotected in a 30% sucrose solution overnight, after which the tissue was mounted in optimal cutting temperature (OCT) and cryosectioned at 20μm. Sections were collected on slides and processed for immunohistochemistry.

**Immunohistochemistry—**Chicken embryonic spinal cords and mouse embryonic spinal cords were sectioned to yield 20μm sections. The details of the antibodies used for immunostaining can be found in the key resources table. Species appropriate Cyanine 3, 5 and Alexa Fluor 488 conjugated secondary antibodies were used (Jackson ImmunoResearch Laboratories). Images were collected on Carl Zeiss LSM700 and LSM800 confocal microscopes.

***In situ* hybridization—***In situ* hybridizations were performed on chicken (HH stage 18–25) and mouse (E11.5) embryonic spinal cords. 3′UTR probes were designed using http://primer3plus.com and verified for specificity to the gene of interest using http://www.ncbi.nlm.nih.gov/tools/primer-blast/.

The chicken and mouse primer sequences used to make *in situ* hybridization probes can be found in key resources table. Probes were made using a DIG RNA labeling kit (Roche, Cat#11175025910). Images were collected on a Carl Zeiss AxioImager M2 fluorescence microscope with an Apotome attachment.

**Western blot analyses—**Cos7 cells were seeded in 12-well or 24 well plates the day before stimulation with netrin1 (R&D, cat# 1109-N1–025) and Bmp4 (Thermo Fisher cat# PHC9534). On the day of stimulation, the cells were starved in FBS-free media for an hour prior to stimulation with 5 ng/mL Bmp4 and 0.5 μg/mL, 0.25 μg/mL or 0.125 μg/mL netrin1. After 1 h of stimulation, the cells were washed with PBS and lysed with RIPA lysis buffer containing a protease inhibitor cocktail (Roche) and the phosphatase inhibitor PhosSTOP (Roche). The cell lysates were kept on ice for 30 min and centrifuged at 20,800×g for 10 min at 4°C. The supernatant was subjected to SDS-PAGE using 10% Tris-Glycine SDS gels followed by transfer onto PVDF membranes (Millipore Sigma). The membranes were blocked using non-fat dry milk (Bio-Rad Laboratories). The blocked membranes were then incubated with the primary antibodies (key resources table) at 4°C overnight. Thereafter, the membranes were washed three times with TBST (20 mM Tris, 150 mM NaCl, 0.1% Tween 20), incubated with species-specific horseradish peroxidase-conjugated secondary antibodies (Jackson ImmunoResearch Laboratories) for an hour at room temperature and then washed again three times with TBST. The chemiluminescent

bands were analyzed using the Pierce Femto Chemiluminescence system on the Azure Imager.

**Mouse embryonic stem cell (mESC) culture and differentiation—**The mouse ESC line MM13[54] was maintained in ESC medium with LIF on mitotically inactive MEFs. Before differentiation, ESC colonies were dissociated, plated on gelatin-coated plates, and allowed to proliferate for 1–2 days. To initiate differentiation, cells were plated on 0.1% gelatin-coated 24-well CellBIND dishes (Corning) with N2/B27 medium containing 10 ng/ml basic fibroblast growth factor (bFGF). On day 1, small colonies of cells can be observed attached to the bottom of the wells. On day 2, cells were supplemented with 10 ng/ml bFGF and 5μM CHIR99021 (Tocris, Cat#4423) for 24 h to induce a neuromesodermal identity.[55] On day 3, cells were directed towards a spinal lineage by exposing them to 100nM RA (Sigma Aldrich, cat# R2625) for 24 h, followed by 100nM RA + 10 ng/ml Bmp4 (Thermo Fisher cat# PHC9534) to induce dorsal spinal cord identity.[25] To evaluate the effects of netrin1 on dI differentiation, two concentrations of mouse recombinant netrin1 (high - 0.5 μg/mL, low - 0.125 μg/mL) (R&D, Cat#1109-N1–025) were added in three different timelines (conditions 1, 2, 3).

For condition 1, netrin1 was added with RA + Bmp4 between day 4 and day 5, resulting in 24 h of netrin1 exposure. For condition 2, netrin1 was added between day 5 and day 6, providing 24 h of netrin1 exposure after the initial patterning by RA + Bmp4. For condition 3, netrin1 was added every other day between day 5 to day 9, leading to an extended 4-day netrin1 exposure. Terminal differentiation was induced by replacing the growth factor containing media with basic N2/B27 medium at day 5, and cultures were allowed to differentiate until day 9. At the end of the differentiation, the cultures were lysed in buffer RLT and RNA was purified using RNAeasy kit (Qiagen, Cat#74104) for preparing cDNA for quantitative reverse transcriptase PCR analysis.

**Reverse transcriptase PCR analysis—**RNA was extracted from at least two independent differentiations using the RNeasy mini purification kit (Qiagen, Cat#74104). cDNA was synthesized using Superscript IV (Thermo Fisher Scientific, Cat#18091050) using oligodT as primers to convert mRNAs into cDNAs. RT-qPCR was always performed in triplicate using SYBR Green Master Mix on a Roche RT-qPCR thermocycler using gene-specific primers (key resources table). The Ct values for each gene were calculated by averaging three technical replicates from independent differentiations for each condition. Expression of the target gene was normalized with the expression of glyceraldehyde-3-phosphaste dehydrogenase (GAPDH) and fold change was calculated using the $2^{-\Delta\Delta Ct}$ method.[79] The variation in fold change in expression is represented in ±SEM (standard error of mean).

**Bulk RNA-Seq and bioinformatic analysis of mESC differentiation cultures treated with recombinant netrin1—**For the bulk RNA-seq analysis, RNA samples were collected from three independent differentiations for day 5 (condition1), and day 6 (condition 2), while two independent differentiations were collected for day 9 (condition3) using an RNAeasy mini kit (Qiagen). Each independent differentiation was started from a distinct vial of mESCs, but the differentiations were run in parallel, to minimize variability.

RNA quality was determined using TapeStation and only samples with >8 RIN score were selected for the library preparations. Libraries were prepared using the Universal Plus mRNA sequencing kit (Tecan) and sequenced on an Illumina Novaseq S2 to obtain a minimum 30–50 million reads/sample.

Reads were obtained as FASTQ files, and the quality of the reads was determined using a FASTQC analysis. The reads were aligned to the mm10 reference mouse genome using the STAR spliced read aligner. Differentially expressed (DE) genes were obtained using the EdgeR[80] and DEseq2[81] packages on R with a selection criteria of False Discovery Rate (FDR $p < 0.05$). The sequencing data were first analyzed for the degree of similarity between the replicates by conducting principal component analysis (PCA) using the top 1000 DE genes. To comprehensively capture the effect of adding netrin1 to the stem cell cultures, we conducted a GO analysis using the rank-less paradigm where all the DE genes (filtered using DESeq2 with FDR<0.05) irrespective of their fold change were subjected to two different GO platforms: Metascape[82] and Enrichr.[83] We obtained similar GO categories from both analyses and the top 10 GO categories were selected for demonstration in Figure 5. For the heatmaps, genes that fall under a specific GO category (e.g., mRNA processing) were identified and their FPKM values were extracted from the DESeq2 result table. The online software, Heatmapper.ca, was used to construct the heatmaps with row scaling normalization. We further performed Gene Set Enrichment Analysis (GSEA)[84] for identifying specific transcription factor targets (Figures 5E and 5F) in our RNA-Seq dataset.

## QUANTIFICATION AND STATISTICAL ANALYSIS

**Quantification—**Chicken experiments: For cell counting quantifications, cell number was counted by hand, and then normalized to a concomitantly performed GFP control electroporation. When quantifying the intensity of the signal, e.g., Smad1/5/8 staining or *Id1/Id3* expression, control and experimental embryos were stained on the same slides to control for background staining. The integrated staining density/intensity was calculated by tracing an area of interest using the lasso tool in ImageJ. The integrated density was corrected for any background staining by subtracting background intensity from the measured integrated density. Areas of interest, such as the domains of Sox2, Atoh1, pSmad1/5/8 staining were quantified by tracing out the area using ImageJ software. The total area of the domains quantified were normalized as a percentage of the total area of the spinal cord to account for variability in total spinal cord area/size. The data is plotted as a fold change in area occupied by the marker. To assess the area of the dorsal vs. ventral spinal cord, the length of the spinal cord was measured along the dorsoventral axis, and then divided into half. Biological replicates: 1–2 chicken embryos per experimental condition were collected within an experiment. Each experiment was repeated at least three times, such that 3–5 embryos were analyzed per experimental condition. Technical replicates: ~10–30 sections were analyzed.

Mouse experiments: Cell counts, areas, and intensity were performed as described for the chicken experiments above. All intensities were corrected for background staining and all areas were normalized to account for variability in total spinal cord size. Cell counts, area and staining intensities were normalized to littermate controls. Biological replicates: 1–2

embryos per experimental condition were collected within an experiment, and embryos were collected from at least three timed pregnancies for a total of 4–5 embryos/condition. Technical replicates: ~10–40 sections were analyzed.

For cell culture experiments, experiments were performed at least 3 independent times. All values were normalized to internal controls.

All quantifications were performed blinded to the experimental condition.

**Statistics—**Data are represented as mean ± SEM (standard error of the mean). Tests for statistical significance were performed using Prism software (version 9). Values of $p < 0.05$ were considered significant in all cases.

## Supplementary Material

Refer to Web version on PubMed Central for supplementary material.

## ACKNOWLEDGMENTS

We would like to thank Lisa Goodrich, Thomas Muller, Bennett Novitch, and Marc Tessier-Lavigne for mouse lines and reagents, and Avihu Klar, Bennett Novitch, Alvaro Sagasti, Larry Zipursky, and the members of the Butler and Novitch laboratories for discussions. One illustration was made using our institutional site license from Biorender.com. This work was supported by a UCLA senior undergraduate research scholarship to K.H.; an undergraduate fellowship on the CSUN CIRM Bridges 3.0 Stem Cell Research & Therapy training program (EDUC2 12718) to C.R.; graduate fellowships from the National Institutes of Health (NIH) (F31 GM007185 and T32 GM7185) and UCLA (Eugene V. Cota-Robles, Whitcome and Hilliard Neurobiology award) to S.A.; a UCLA Whitcome and NSF (DGE-2034835) graduate fellowship to Y.M.-A.; a UCLA Broad Stem Cell Research Center (BSCRC) postdoctoral training grant to S.G.; a grant from the NIH (P50 HD103557) to R.K.; and NIH grants (R01 NS123187, R01 NS085097, and P50 HD103557) and innovation awards from the BSCRC to S.J.B.

## REFERENCES

1. Kennedy TE, Serafini T, de la Torre JR, and Tessier-Lavigne M. (1994). Netrins are diffusible chemotropic factors for commissural axons in the embryonic spinal cord. Cell 78, 425–435. [PubMed: 8062385]
2. Serafini T, Kennedy TE, Galko MJ, Mirzayan C, Jessell TM, and Tessier-Lavigne M. (1994). The netrins define a family of axon outgrowth-promoting proteins homologous to C. elegans UNC-6. Cell 78, 409–424. [PubMed: 8062384]
3. Deiner MS, Kennedy TE, Fazeli A, Serafini T, Tessier-Lavigne M, and Sretavan DW (1997). Netrin-1 and DCC mediate axon guidance locally at the optic disc: loss of function leads to optic nerve hypoplasia. Neuron 19, 575–589. [PubMed: 9331350]
4. Hamasaki T, Goto S, Nishikawa S, and Ushio Y. (2001). A role of netrin-1 in the formation of the subcortical structure striatum: repulsive action on the migration of late-born striatal neurons. J. Neurosci. 21, 4272–4280. 10.1523/JNEUROSCI.21-12-04272.2001. [PubMed: 11404412]
5. Livesey FJ, and Hunt SP (1997). Netrin and netrin receptor expression in the embryonic mammalian nervous system suggests roles in retinal, striatal, nigral, and cerebellar development. Mol. Cell. Neurosci. 8, 417–429. 10.1006/mcne.1997.0598. [PubMed: 9143559]
6. Liu Y, Stein E, Oliver T, Li Y, Brunken WJ, Koch M, Tessier-Lavigne M, and Hogan BLM (2004). Novel role for Netrins in regulating epithelial behavior during lung branching morphogenesis. Curr. Biol. 14, 897–905. 10.1016/j.cub.2004.05.020. [PubMed: 15186747]
7. Shin SK, Nagasaka T, Jung BH, Matsubara N, Kim WH, Carethers JM, Boland CR, and Goel A. (2007). Epigenetic and genetic alterations in Netrin-1 receptors UNC5C and DCC in human colon cancer. Gastroenterology 133, 1849–1857. 10.1053/j.gastro.2007.08.074. [PubMed: 18054557]

8. Srinivasan K, Strickland P, Valdes A, Shin GC, and Hinck L. (2003). Netrin-1/neogenin interaction stabilizes multipotent progenitor cap cells during mammary gland morphogenesis. Dev. Cell 4, 371–382. 10.1016/s1534-5807(03)00054-6. [PubMed: 12636918]

9. Yebra M, Montgomery AMP, Diaferia GR, Kaido T, Silletti S, Perez B, Just ML, Hildbrand S, Hurford R, Florkiewicz E, et al. (2003). Recognition of the neural chemoattractant Netrin-1 by integrins alpha6beta4 and alpha3beta1 regulates epithelial cell adhesion and migration. Dev. Cell 5, 695–707. 10.1016/s1534-5807(03)00330-7. [PubMed: 14602071]

10. Zhang J, and Cai H. (2010). Netrin-1 prevents ischemia/reperfusion-induced myocardial infarction via a DCC/ERK1/2/eNOS s1177/NO/DCC feed-forward mechanism. J. Mol. Cell. Cardiol. 48, 1060–1070. 10.1016/j.yjmcc.2009.11.020. [PubMed: 20004665]

11. Andrews MG, Kong J, Novitch BG, and Butler SJ (2019). New perspectives on the mechanisms establishing the dorsal-ventral axis of the spinal cord. Curr. Top. Dev. Biol. 132, 417–450. 10.1016/bs.ctdb.2018.12.010. [PubMed: 30797516]

12. Gupta S, and Butler SJ (2021). Getting in touch with your senses: Mechanisms specifying sensory interneurons in the dorsal spinal cord. WIREs Mech. Dis. 13, e1520. 10.1002/wsbm.1520. [PubMed: 34730293]

13. Liem KF Jr., Tremml G, and Jessell TM (1997). A role for the roof plate and its resident TGFbeta-related proteins in neuronal patterning in the dorsal spinal cord. Cell 91, 127–138. [PubMed: 9335341]

14. Butler SJ, and Dodd J. (2003). A role for BMP heterodimers in roof plate-mediated repulsion of commissural axons. Neuron 38, 389–401. [PubMed: 12741987]

15. Lee KJ, Dietrich P, and Jessell TM (2000). Genetic ablation reveals that the roof plate is essential for dorsal interneuron specification. Nature 403, 734–740. [PubMed: 10693795]

16. Lee KJ, Mendelsohn M, and Jessell TM (1998). Neuronal patterning by BMPs: a requirement for GDF7 in the generation of a discrete class of commissural interneurons in the mouse spinal cord. Genes Dev. 12, 3394–3407. [PubMed: 9808626]

17. Wine-Lee L, Ahn KJ, Richardson RD, Mishina Y, Lyons KM, and Crenshaw EB 3rd. (2004). Signaling through BMP type 1 receptors is required for development of interneuron cell types in the dorsal spinal cord. Development 131, 5393–5403. [PubMed: 15469980]

18. Andrews MG, Del Castillo LM, Ochoa-Bolton E, Yamauchi K, Smogorzewski J, and Butler SJ (2017). BMPs direct sensory interneuron identity in the developing spinal cord using signal-specific not morphogenic activities. Elife 6, e30647. 10.7554/eLife.30647.

19. Le Dreau G, Garcia-Campmany L, Rabadan MA, Ferronha T, Tozer S, Briscoe J, and Marti E. (2012). Canonical BMP7 activity is required for the generation of discrete neuronal populations in the dorsal spinal cord. Development 139, 259–268. [PubMed: 22159578]

20. Yamauchi K, Phan KD, and Butler SJ (2008). BMP type I receptor complexes have distinct activities mediating cell fate and axon guidance decisions. Development 135, 1119–1128. [PubMed: 18272594]

21. Shi Y, and Massagué J. (2003). Mechanisms of TGF-beta signaling from cell membrane to the nucleus. Cell 113, 685–700. [PubMed: 12809600]

22. Hazen VM, Andrews MG, Umans L, Crenshaw EB 3rd, Zwijsen A, and Butler SJ (2012). BMP receptor-activated Smads direct diverse functions during the development of the dorsal spinal cord. Dev. Biol. 367, 216–227. [PubMed: 22609550]

23. Novitch BG, Wichterle H, Jessell TM, and Sockanathan S. (2003). A requirement for retinoic acid-mediated transcriptional activation in ventral neural patterning and motor neuron specification. Neuron 40, 81–95. [PubMed: 14527435]

24. Diez del Corral R, Olivera-Martinez I, Goriely A, Gale E, Maden M, and Storey K. (2003). Opposing FGF and retinoid pathways control ventral neural pattern, neuronal differentiation, and segmentation during body axis extension. Neuron 40, 65–79. [PubMed: 14527434]

25. Gupta S, Kawaguchi R, Heinrichs E, Gallardo S, Castellanos S, Mandric I, Novitch BG, and Butler SJ (2022). In vitro atlas of dorsal spinal interneurons reveals Wnt signaling as a critical regulator of progenitor expansion. Cell Rep. 40, 111119. 10.1016/j.celrep.2022.111119.

26. Alvarez S, Varadarajan SG, and Butler SJ (2021). Dorsal commissural axon guidance in the developing spinal cord. Curr. Top. Dev. Biol. 142, 197–231. 10.1016/bs.ctdb.2020.10.009. [PubMed: 33706918]
27. Yamauchi K, Yamazaki M, Abe M, Sakimura K, Lickert H, Kawasaki T, Murakami F, and Hirata T. (2017). Netrin-1 Derived from the Ventricular Zone, but not the Floor Plate, Directs Hindbrain Commissural Axons to the Ventral Midline. Sci. Rep. 7, 11992. 10.1038/s41598-017-12269-8. [PubMed: 28931893]
28. Dominici C, Moreno-Bravo JA, Puiggros SR, Rappeneau Q, Rama N, Vieugue P, Bernet A, Mehlen P, and Chédotal A. (2017). Floor-plate-derived netrin-1 is dispensable for commissural axon guidance. Nature 545, 350–354. 10.1038/nature22331. [PubMed: 28445456]
29. Varadarajan SG, Kong JH, Phan KD, Kao TJ, Panaitof SC, Cardin J, Eltzschig H, Kania A, Novitch BG, and Butler SJ (2017). Netrin1 Produced by Neural Progenitors, Not Floor Plate Cells, Is Required for Axon Guidance in the Spinal Cord. Neuron 94, 790–799.e3. 10.1016/j.neuron.2017.03.007. [PubMed: 28434801]
30. Varadarajan SG, and Butler SJ (2017). Netrin1 establishes multiple boundaries for axon growth in the developing spinal cord. Dev. Biol. 430, 177–187. 10.1016/j.ydbio.2017.08.001. [PubMed: 28780049]
31. Mehlen P, and Guenebeaud C. (2010). Netrin-1 and its dependence receptors as original targets for cancer therapy. Curr. Opin. Oncol. 22, 46–54. 10.1097/CCO.0b013e328333dcd1. [PubMed: 19934758]
32. Ramesh G, Berg A, and Jayakumar C. (2011). Plasma netrin-1 is a diagnostic biomarker of human cancers. Biomarkers 16, 172–180. 10.3109/1354750X.2010.541564. [PubMed: 21303223]
33. Delloye-Bourgeois C, Brambilla E, Coissieux MM, Guenebeaud C, Pedeux R, Firlej V, Cabon F, Brambilla C, Mehlen P, and Bernet A. (2009). Interference with netrin-1 and tumor cell death in non-small cell lung cancer. J. Natl. Cancer Inst. 101, 237–247. 10.1093/jnci/djn491. [PubMed: 19211441]
34. Delloye-Bourgeois C, Fitamant J, Paradisi A, Cappellen D, Douc-Rasy S, Raquin MA, Stupack D, Nakagawara A, Rousseau R, Combaret V, et al. (2009). Netrin-1 acts as a survival factor for aggressive neuroblastoma. J. Exp. Med. 206, 833–847. 10.1084/jem.20082299. [PubMed: 19349462]
35. Kefeli U, Ucuncu Kefeli A, Cabuk D, Isik U, Sonkaya A, Acikgoz O, Ozden E, and Uygun K. (2017). Netrin-1 in cancer: Potential biomarker and therapeutic target? Tumour Biol. 39, 1010428317698388. 10.1177/1010428317698388.
36. Toque HA, Fernandez-Flores A, Mohamed R, Caldwell RB, Ramesh G, and Caldwell RW (2017). Netrin-1 is a novel regulator of vascular endothelial function in diabetes. PLoS One 12, e0186734. 10.1371/journal.pone.0186734.
37. Paradisi A, Maisse C, Coissieux MM, Gadot N, Lépinasse F, Delloye-Bourgeois C, Delcros JG, Svrcek M, Neufert C, Fléjou JF, et al. (2009). Netrin-1 up-regulation in inflammatory bowel diseases is required for colorectal cancer progression. Proc. Natl. Acad. Sci. USA 106, 17146–17151. 10.1073/pnas.0901767106. [PubMed: 19721007]
38. Sato T, Kokabu S, Enoki Y, Hayashi N, Matsumoto M, Nakahira M, Sugasawa M, and Yoda T. (2017). Functional Roles of Netrin-1 in Osteoblast Differentiation. In Vivo 31, 321–328. 10.21873/in-vivo.11062. [PubMed: 28438858]
39. Strizzi L, Mancino M, Bianco C, Raafat A, Gonzales M, Booth BW, Watanabe K, Nagaoka T, Mack DL, Howard B, et al. (2008). Netrin-1 can affect morphogenesis and differentiation of the mouse mammary gland. J. Cell. Physiol. 216, 824–834. 10.1002/jcp.21462. [PubMed: 18425773]
40. Mancino M, Esposito C, Watanabe K, Nagaoka T, Gonzales M, Bianco C, Normanno N, Salomon DS, and Strizzi L. (2009). Neuronal guidance protein Netrin-1 induces differentiation in human embryonal carcinoma cells. Cancer Res. 69, 1717–1721. 10.1158/0008-5472.CAN-08-2985. [PubMed: 19223540]
41. Abdullah A, Herdenberg C, and Hedman H. (2021). Netrin-1 functions as a suppressor of bone morphogenetic protein (BMP) signaling. Sci. Rep. 11, 8585. 10.1038/s41598-021-87949-7. [PubMed: 33883596]

42. Miyazono K, and Miyazawa K. (2002). Id: a target of BMP signaling. Sci. STKE 2002, pe40. 10.1126/stke.2002.151.pe40. [PubMed: 12297674]
43. Jen Y, Weintraub H, and Benezra R. (1992). Overexpression of Id protein inhibits the muscle differentiation program: in vivo association of Id with E2A proteins. Genes Dev. 6, 1466–1479. [PubMed: 1644289]
44. Lyden D, Young AZ, Zagzag D, Yan W, Gerald W, O'Reilly R, Bader BL, Hynes RO, Zhuang Y, Manova K, and Benezra R. (1999). Id1 and Id3 are required for neurogenesis, angiogenesis and vascularization of tumour xenografts. Nature 401, 670–677. [PubMed: 10537105]
45. Yokota Y. (2001). Id and development. Oncogene 20, 8290–8298. [PubMed: 11840321]
46. Sikder HA, Devlin MK, Dunlap S, Ryu B, and Alani RM (2003). Id proteins in cell growth and tumorigenesis. Cancer Cell 3, 525–530. [PubMed: 12842081]
47. Ruzinova MB, and Benezra R. (2003). Id proteins in development, cell cycle and cancer. Trends Cell Biol. 13, 410–418. [PubMed: 12888293]
48. Hemmati-Brivanlou A, and Thomsen GH (1995). Ventral mesodermal patterning in Xenopus embryos: expression patterns and activities of BMP-2 and BMP-4. Dev. Genet. 17, 78–89. 10.1002/dvg.1020170109. [PubMed: 7554498]
49. Zou H, and Niswander L. (1996). Requirement for BMP signaling in interdigital apoptosis and scale formation. Science 272, 738–741. [PubMed: 8614838]
50. Kobayashi T, Lyons KM, McMahon AP, and Kronenberg HM (2005). BMP signaling stimulates cellular differentiation at multiple steps during cartilage development. Proc. Natl. Acad. Sci. USA 102, 18023–18027. 10.1073/pnas.0503617102. [PubMed: 16322106]
51. Wang H, Copeland NG, Gilbert DJ, Jenkins NA, and Tessier-Lavigne M. (1999). Netrin-3, a mouse homolog of human NTN2L, is highly expressed in sensory ganglia and shows differential binding to netrin receptors. J. Neurosci. 19, 4938–4947. [PubMed: 10366627]
52. Alexopoulou AN, Couchman JR, and Whiteford JR (2008). The CMV early enhancer/ chicken beta actin (CAG) promoter can be used to drive transgene expression during the differentiation of murine embryonic stem cells into vascular progenitors. BMC Cell Biol. 9, 2. 10.1186/1471-2121-9-2. [PubMed: 18190688]
53. Alaynick WA, Jessell TM, and Pfaff SL (2011). SnapShot: spinal cord development. Cell 146, 178–178.e1. [PubMed: 21729788]
54. Wichterle H, Lieberam I, Porter JA, and Jessell TM (2002). Directed differentiation of embryonic stem cells into motor neurons. Cell 110, 385–397. [PubMed: 12176325]
55. Gouti M, Tsakiridis A, Wymeersch FJ, Huang Y, Kleinjung J, Wilson V, and Briscoe J. (2014). In vitro generation of neuromesodermal progenitors reveals distinct roles for wnt signalling in the specification of spinal cord and paraxial mesoderm identity. PLoS Biol. 12, e1001937. 10.1371/ journal.pbio.1001937.
56. Gupta S, Sivalingam D, Hain S, Makkar C, Sosa E, Clark A, and Butler SJ (2018). Deriving Dorsal Spinal Sensory Interneurons from Human Pluripotent Stem Cells. Stem Cell Rep. 10, 390–405. 10.1016/j.stemcr.2017.12.012.
57. Gupta S, Heinrichs E, Novitch BG, and Butler SJ (2024). Investigating the basis of lineage decisions and developmental trajectories in the dorsal spinal cord through pseudotime analyses. Preprint at bioRxiv. 10.1101/2023.07.24.550380.
58. Serafini T, Colamarino SA, Leonardo ED, Wang H, Beddington R, Skarnes WC, and Tessier-Lavigne M. (1996). Netrin-1 is required for commissural axon guidance in the developing vertebrate nervous system. Cell 87, 1001–1014. [PubMed: 8978605]
59. Kennedy TE, Wang H, Marshall W, and Tessier-Lavigne M. (2006). Axon guidance by diffusible chemoattractants: a gradient of netrin protein in the developing spinal cord. J. Neurosci. 26, 8866–8874. 10.1523/JNEUROSCI.5191-05.2006. [PubMed: 16928876]
60. Yung AR, Nishitani AM, and Goodrich LV (2015). Phenotypic analysis of mice completely lacking netrin 1. Development 142, 3686–3691. 10.1242/dev.128942. [PubMed: 26395479]
61. Glasgow SM, Henke RM, Macdonald RJ, Wright CVE, and Johnson JE (2005). Ptf1a determines GABAergic over glutamatergic neuronal cell fate in the spinal cord dorsal horn. Development 132, 5461–5469. [PubMed: 16291784]

62. Novitch BG, Chen AI, and Jessell TM (2001). Coordinate regulation of motor neuron subtype identity and pan-neuronal properties by the bHLH repressor Olig2. Neuron 31, 773–789. [PubMed: 11567616]
63. Lee KY, Jeong JW, Wang J, Ma L, Martin JF, Tsai SY, Lydon JP, and DeMayo FJ (2007). Bmp2 is critical for the murine uterine decidual response. Mol. Cell Biol. 27, 5468–5478. 10.1128/MCB.00342-07. [PubMed: 17515606]
64. Chiba N, Noguchi Y, Seong CH, Ohnishi T, and Matsuguchi T. (2022). EGR1 plays an important role in BMP9-mediated osteoblast differentiation by promoting SMAD1/5 phosphorylation. FEBS Lett. 596, 1720–1732. 10.1002/1873-3468.14407. [PubMed: 35594155]
65. Thapar R. (2015). Roles of Prolyl Isomerases in RNA-Mediated Gene Expression. Biomolecules 5, 974–999. 10.3390/biom5020974. [PubMed: 25992900]
66. Benecke H, Lührmann R, and Will CL (2005). The U11/U12 snRNP 65K protein acts as a molecular bridge, binding the U12 snRNA and U11–59K protein. EMBO J. 24, 3057–3069. 10.1038/sj.emboj.7600765. [PubMed: 16096647]
67. Timmer JR, Wang C, and Niswander L. (2002). BMP signaling patterns the dorsal and intermediate neural tube via regulation of homeobox and helix-loop-helix transcription factors. Development 129, 2459–2472. [PubMed: 11973277]
68. Wang RN, Green J, Wang Z, Deng Y, Qiao M, Peabody M, Zhang Q, Ye J, Yan Z, Denduluri S, et al. (2014). Bone Morphogenetic Protein (BMP) signaling in development and human diseases. Genes Dis. 1, 87–105. 10.1016/j.gendis.2014.07.005. [PubMed: 25401122]
69. Le Dreau G. (2021). BuMPing Into Neurogenesis: How the Canonical BMP Pathway Regulates Neural Stem Cell Divisions Throughout Space and Time. Front. Neurosci. 15, 819990. 10.3389/fnins.2021.819990.
70. Brazil DP, Church RH, Surae S, Godson C, and Martin F. (2015). BMP signalling: agony and antagony in the family. Trends Cell Biol. 25, 249–264. 10.1016/j.tcb.2014.12.004. [PubMed: 25592806]
71. Kim S, and Martin KC (2015). Neuron-wide RNA transport combines with netrin-mediated local translation to spatially regulate the synaptic proteome. Elife 4, e04158. 10.7554/eLife.04158.
72. Nakao A, Afrakhte M, Morén A, Nakayama T, Christian JL, Heuchel R, Itoh S, Kawabata M, Heldin NE, Heldin CH, and ten Dijke P. (1997). Identification of Smad7, a TGFbeta-inducible antagonist of TGF-beta signalling. Nature 389, 631–635. 10.1038/39369. [PubMed: 9335507]
73. Hazen VM, Phan KD, Hudiburgh S, and Butler SJ (2011). Inhibitory Smads differentially regulate cell fate specification and axon dynamics in the dorsal spinal cord. Dev. Biol. 356, 566–575. [PubMed: 21718693]
74. Fazeli A, Dickinson SL, Hermiston ML, Tighe RV, Steen RG, Small CG, Stoeckli ET, Keino-Masu K, Masu M, Rayburn H, et al. (1997). Phenotype of mice lacking functional Deleted in colorectal cancer (Dcc) gene. Nature 386, 796–804. [PubMed: 9126737]
75. Phan KD, Croteau LP, Kam JWK, Kania A, Cloutier JF, and Butler SJ (2011). Neogenin may functionally substitute for Dcc in chicken. PLoS One 6, e22072. 10.1371/journal.pone.0022072.
76. Müller T, Anlag K, Wildner H, Britsch S, Treier M, and Birchmeier C. (2005). The bHLH factor Olig3 coordinates the specification of dorsal neurons in the spinal cord. Genes Dev 19, 733–743. 10.1101/gad.326105. [PubMed: 15769945]
77. Helms AW, and Johnson JE (1998). Progenitors of dorsal commissural interneurons are defined by MATH1 expression. Development 125, 919–928. 10.1242/dev.125.5.919. [PubMed: 9449674]
78. Miyazaki J, Takaki S, Araki K, Tashiro F, Tominaga A, Takatsu K, and Yamamura K. (1989). Expression vector system based on the chicken beta-actin promoter directs efficient production of interleukin-5. Gene 79, 269–277. [PubMed: 2551778]
79. Livak KJ, and Schmittgen TD (2001). Analysis of relative gene expression data using real-time quantitative PCR and the 2(-Delta Delta C(T)) Method. Methods 25, 402–408. 10.1006/meth.2001.1262. [PubMed: 11846609]
80. Robinson MD, McCarthy DJ, and Smyth GK (2010). edgeR: a Bioconductor package for differential expression analysis of digital gene expression data. Bioinformatics 26, 139–140. 10.1093/bioinformatics/btp616. [PubMed: 19910308]

81. Love MI, Huber W, and Anders S. (2014). Moderated estimation of fold change and dispersion for RNA-seq data with DESeq2. Genome Biol. 15, 550. 10.1186/s13059-014-0550-8. [PubMed: 25516281]

82. Zhou Y, Zhou B, Pache L, Chang M, Khodabakhshi AH, Tanaseichuk O, Benner C, and Chanda SK (2019). Metascape provides a biologist-oriented resource for the analysis of systems-level datasets. Nat. Commun. 10, 1523. 10.1038/s41467-019-09234-6. [PubMed: 30944313]

83. Chen EY, Tan CM, Kou Y, Duan Q, Wang Z, Meirelles GV, Clark NR, and Ma'ayan A. (2013). Enrichr: interactive and collaborative HTML5 gene list enrichment analysis tool. BMC Bioinf. 14, 128. 10.1186/1471-2105-14-128.

84. Subramanian A, Tamayo P, Mootha VK, Mukherjee S, Ebert BL, Gillette MA, Paulovich A, Pomeroy SL, Golub TR, Lander ES, and Mesirov JP (2005). Gene set enrichment analysis: a knowledge-based approach for interpreting genome-wide expression profiles. Proc. Natl. Acad. Sci. USA 102, 15545–15550. 10.1073/pnas.0506580102. [PubMed: 16199517]

## Highlights

- Netrin1 is present in the immediate spinal cord, adjacent to the domain of Bmp signaling
- Modulating netrin1 levels alters the number of dorsal progenitors and interneurons (dIs)
- The gain or loss of netrin1 modifies the level of Bmp signaling and its downstream targets
- Netrin1 regulates mRNA processing to restrict Bmp signaling to the dorsal-most spinal cord

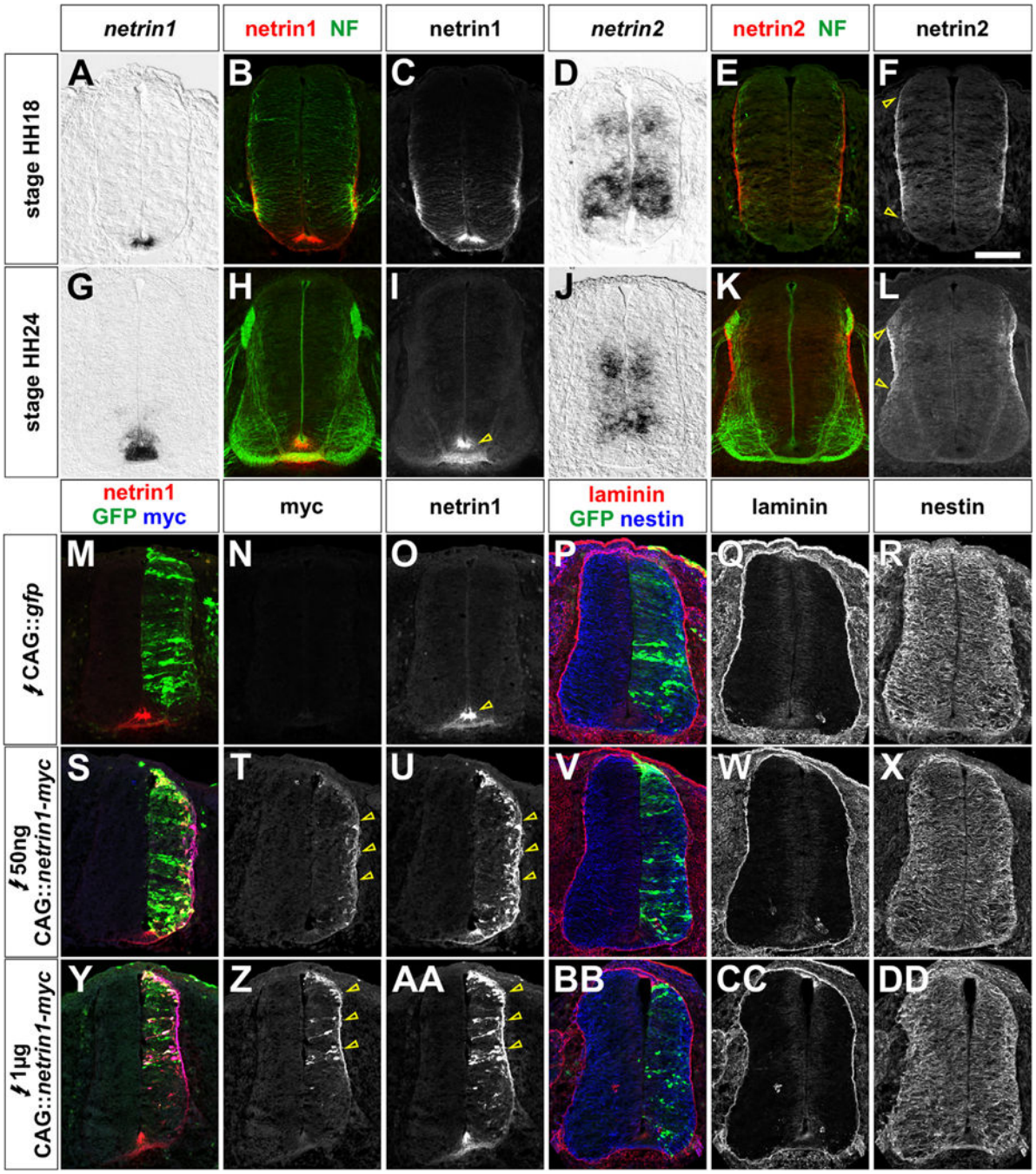


**Figure 1. Overexpression of netrin1 does not affect the integrity of the developing spinal cord**

(A–L) Distribution of netrin1 (A–C and G–I) and netrin2 in (D–F and J–L) in thoracic sections of the HH18 (A–F) and HH24 (G–L) spinal cord. *Netrin1* mRNA is expressed in the apical FP (A and G), while netrin1 protein (red, B and H) decorates the apical-most and basal FP (arrowhead, C and I), where it is coincident with $NF^+$ axons crossing the FP (H). *Netrin2* mRNA is expressed in the intermediate VZ (D and J), while netrin2 protein (red, E and K) decorates pial surface in the intermediate spinal cord (arrowheads, F and L), immediately adjacent to $NF^+$ axons (green) extending ventrally in the dorsal spinal cord (L).

(M–R) Electroporation of a control fluorophore, GFP (green, M and P), expressed from a ubiquitously expressed CAG enhancer, does not affect the distribution of endogenous netrin1 (red, M; arrowhead, O), or the integrity of the spinal cord as assessed by antibodies against laminin (red, P and Q) and nestin (blue, P and R). (S–DD) In contrast, electroporation of a low (50 ng, S–X) or high (1 μg, Y–DD) concentration of netrin1-myc construct, results in ectopic netrin1 (red, S, Y, U, and AA) and myc (blue, S, Y, T, and Z) decorating the pial surface (arrowheads, T, U, Z, and AA) with no effect on the distribution of laminin (red, V, W, BB, and CC) or nestin (blue, V, X, BB, and DD). Scale bar: 100 μm.

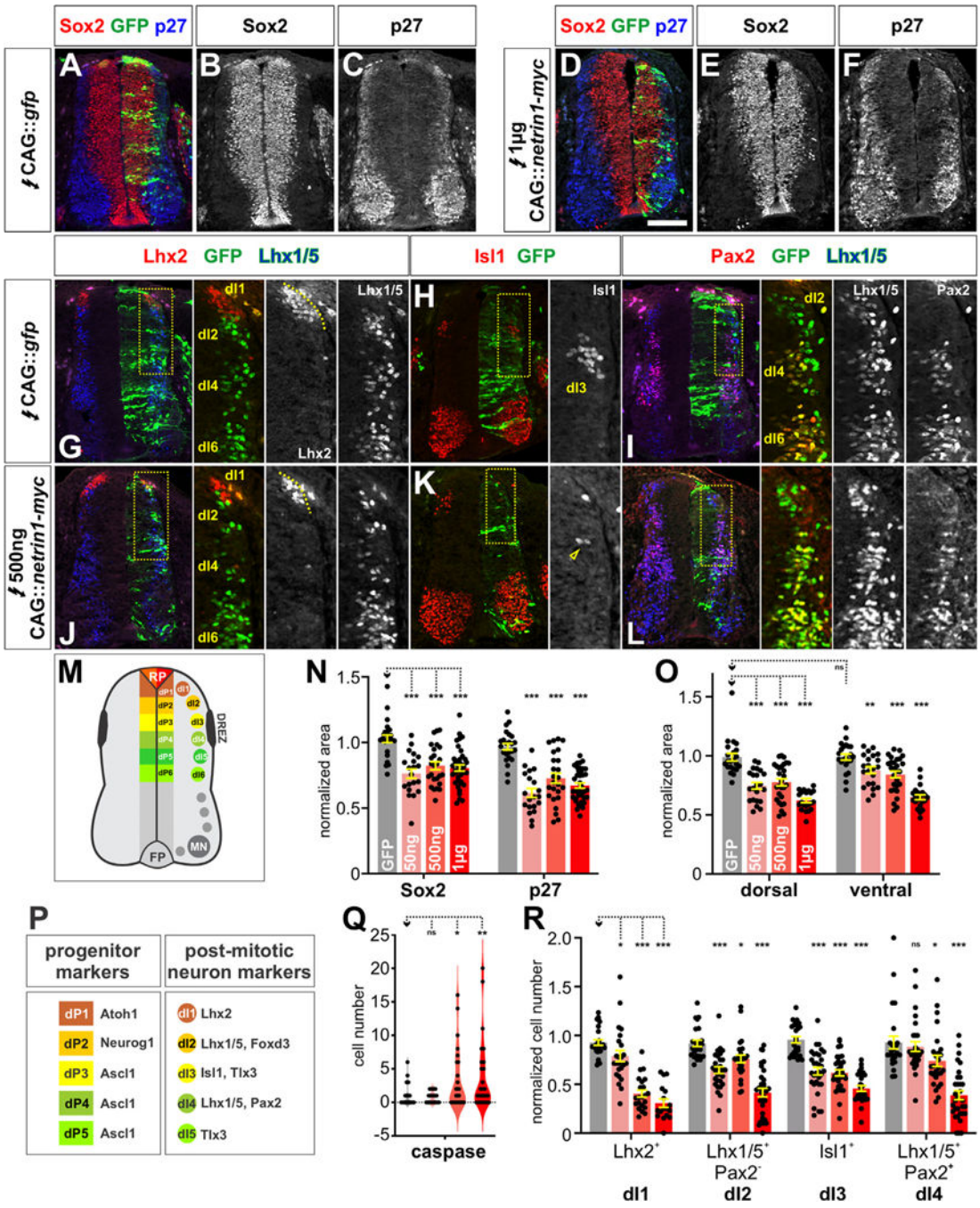


**Figure 2. Overexpression of ntrin1 in chicken embryos results in the loss of dorsal interneurons**

(A–L) Chicken spinal cords were electroporated at HH stage 14 with *Gfp* (A–C and G–I) or different concentrations of *netrin1* (50 ng, 500 ng, 1 µg) (D–F and J–L) under the control of the CAG enhancer and incubated until HH stage 24. Thoracic transverse sections were labeled with antibodies against Sox2 (red, A, B, D, and E), p27 (blue, A, C, D, and F), Lhx2 (red, G and J), Isl (red, H and K), Lhx1/5 (blue/green G, I, J, and L) and Pax2 (red, I and L). The dotted box (G–L) indicates the magnified region in the adjacent panel(s).

(M) Schematic spinal cord, showing the position of the dorsal progenitor (dP) domains and post-mitotic dorsal interneurons (dIs).

(N and O) Ectopic *Gfp* expression had no significant effect on cell fate specification. In contrast the total area occupied by $Sox2^+$ (progenitors) or $p27^+$ (neurons) cells was significantly reduced at all concentrations of netrin1 tested (N). The dorsal spinal cord was more profoundly affected at lower concentrations of netrin1 than the ventral spinal cord (O). $n > 20$ sections from four embryos from each experimental condition (i.e., GFP, 50 ng, 500 ng, and 1 μg netrin), Student's t test. (P) The different classes of dIs can be identified by specific combinations of transcription factors.

(Q) There was no significant difference ($p > 0.58$) in the number of $caspase^+$ cells between spinal cords electroporated with GFP and 50 ng of netrin1. In contrast, there was significant cell death when the higher concentrations of netrin1 were electroporated. $n > 20$ sections from four embryos from each condition (GFP, 50 ng, 500 ng, and 1 μg netrin). Student's t test.

(R) Ectopic *Gfp* expression had no significant effect on dI specification. However, all concentrations of netrin1 tested significantly reduced the number of $Lhx2^+$ dI1s, $Lhx1/5^+$ $Pax2^-$ dI2s, and $Isl1^+$ dI3s in a dose-dependent manner. In contrast, only the higher concentrations of netrin1 reduced the number of $Lhx1/5^+$ $Pax2^+$ dI4s. $n > 20$ sections from six embryos from each condition (GFP, 50 ng, 500 ng, and 1 μg netrin), one way ANOVA. Probability of similarity between control and experimental groups: $*p < 0.05$, $**p < 0.005$ $***p < 0.0005$. Scale bar: 100 μm.

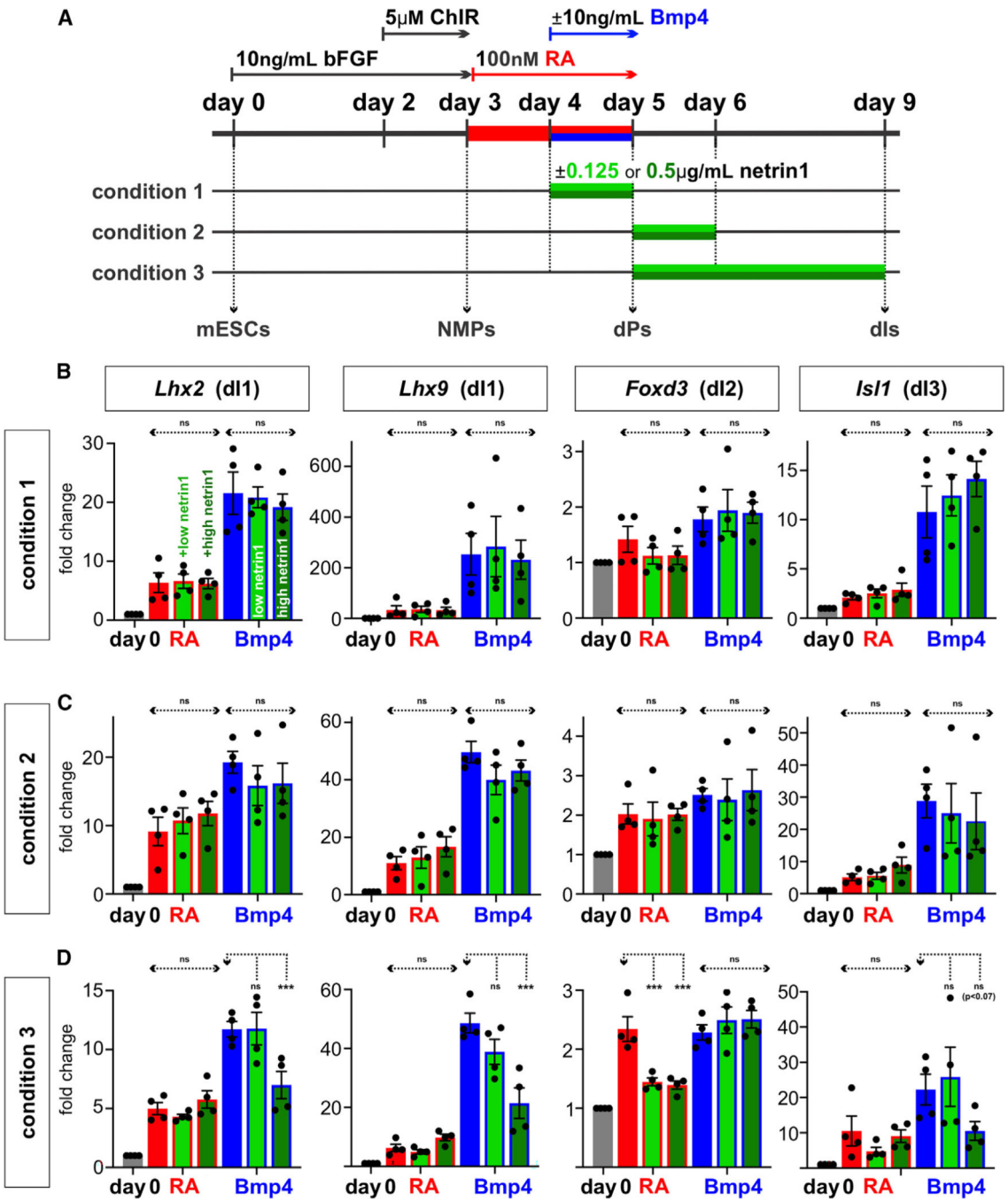


**Figure 3. Addition of netrin1 blocks dorsalization in mESC stem cell model of dI differentiation**

(A) Two concentrations of Netrin1 recombinant protein (0.125 μg/mL [low] and 0.5 μg/mL [high]) were added to the RA ± Bmp4 protocol at the same time as Bmp4 from day 4–5 (condition 1), immediately after Bmp4 treatment from day 5–6 (condition 2), and for an extended period after Bmp4 treatment from day 5–9 (condition 3). qPCR was used to assess alterations in gene expression.

(B and C) The addition of either high (dark green) or low (light green) netrin1 in condition 1 and 2 had no significant effect on the expression of *Lhx2* and *Lhx9* (dI1), *Foxd3* (dI2), or *Isl1* (dI3) compared to RA (red) or RA + Bmp4 (blue) controls.
(D) Prolonged treatment with 0.5 μg/mL netrin1 in the RA + Bmp4 protocol significantly reduced the expression of both dI1 markers, and there is a trend ($p < 0.07$) toward the loss of dI3 marker *Isl1*. Probability of similarity between control and experimental groups: $*p < 0.05$.

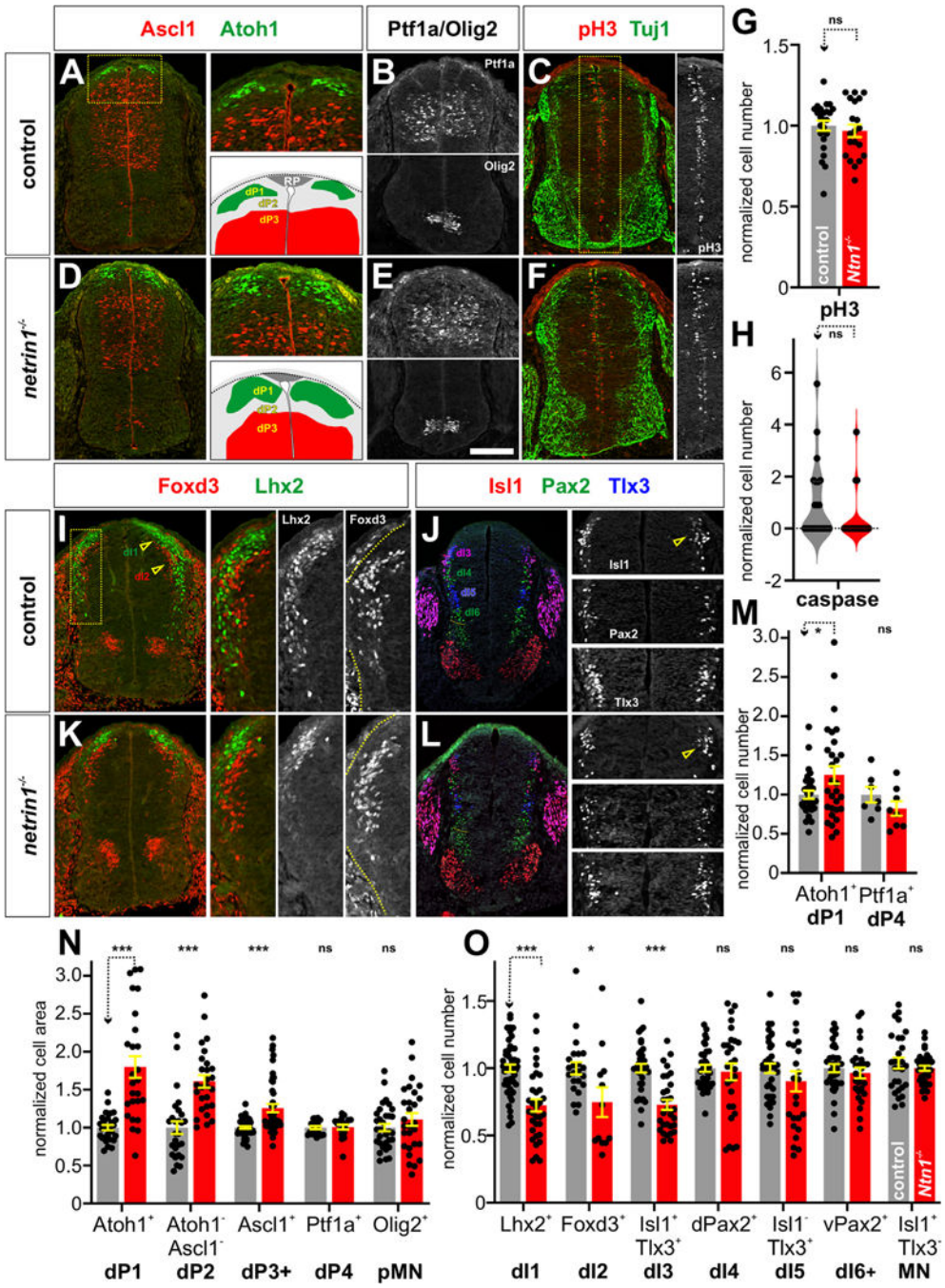


**Figure 4. Netrin1 is required to limit the number of the dorsal-most NPCs**

(A–F) Thoracic transverse spinal cord sections from either control (A–C) or *netrin1*$^{-/-}$ (D–F). E11.5 mouse spinal cords were labeled with antibodies against Ascl1 (A and D; red, dP3–dP5), Atohl1 (A and D; green, dP1), Ptf1a (top panel, B and E; dP4), Olig2 (bottom panel, B and E; pMN), phospho-histone H3 (C and F; red; cells in mitosis [M] phase), and Tuj1 (C and F; green; neurites). The dotted box in (A) and (C) indicates position of the magnified region in the adjacent panel(s).

(G and H) There was no significant difference in the number of cells in M phase (G, $p > 0.50$; $n = >20$ sections from three control and three *netrin1*$^{-/-}$ embryos) or that were caspase$^{+}$ (i.e., dying) (H, $p > 0.28$; $n = >13$ sections from three control and three *netrin1*$^{-/-}$ embryos) between control and *netrin1*$^{-/-}$ spinal cords.

(I–L) To assess for changes in post-mitotic dIs, thoracic transverse spinal cord sections from either control (I and J) or *netrin1*$^{-/-}$ (K and L) E11.5 mouse spinal cords were labeled with antibodies against Lhx2 (I and K; green; dI1), Foxd3 (I and K; red; dI2), Isl (J and L; red, dI3, MNs), Pax2 (J and L; green; dI4, dI6, v0), and Tlx3 (J and L; blue; dI3, dI5). The dotted box (I–L) indicates the magnified region in the adjacent panel(s).

(M and N) Loss of netrin1 resulted in a 25% increase in the number of Atoh1$^{+}$ dP1s and an almost 2-fold increase in the area occupied by the dP1s. Similarly, the area of the dP2 domain (region bounded by the Atoh1$^{+}$ and Ascl1$^{+}$ domains) was increased by 60%, and the Ascl1$^{+}$ dP3-dP5 domain was increased by 25%. In contrast, there was no change in the area of the Ptf1a$^{+}$ dP4 domain ($n > 26$ sections from four embryos).

(O) This increased number of progenitors did not result in a loss of dIs. Rather there was a ~30% decrease specifically in the number of dI1, dI2, and dI3s ($n > 25$ sections from five embryos) but not in the intermediate dorsal populations or the ventral motor neurons (MNs). Probability of similarity between control and experimental groups: *$p < 0.05$, **$p < 0.005$, ***$p < 0.0005$; Student's t test. Scale bar: 100 μm.

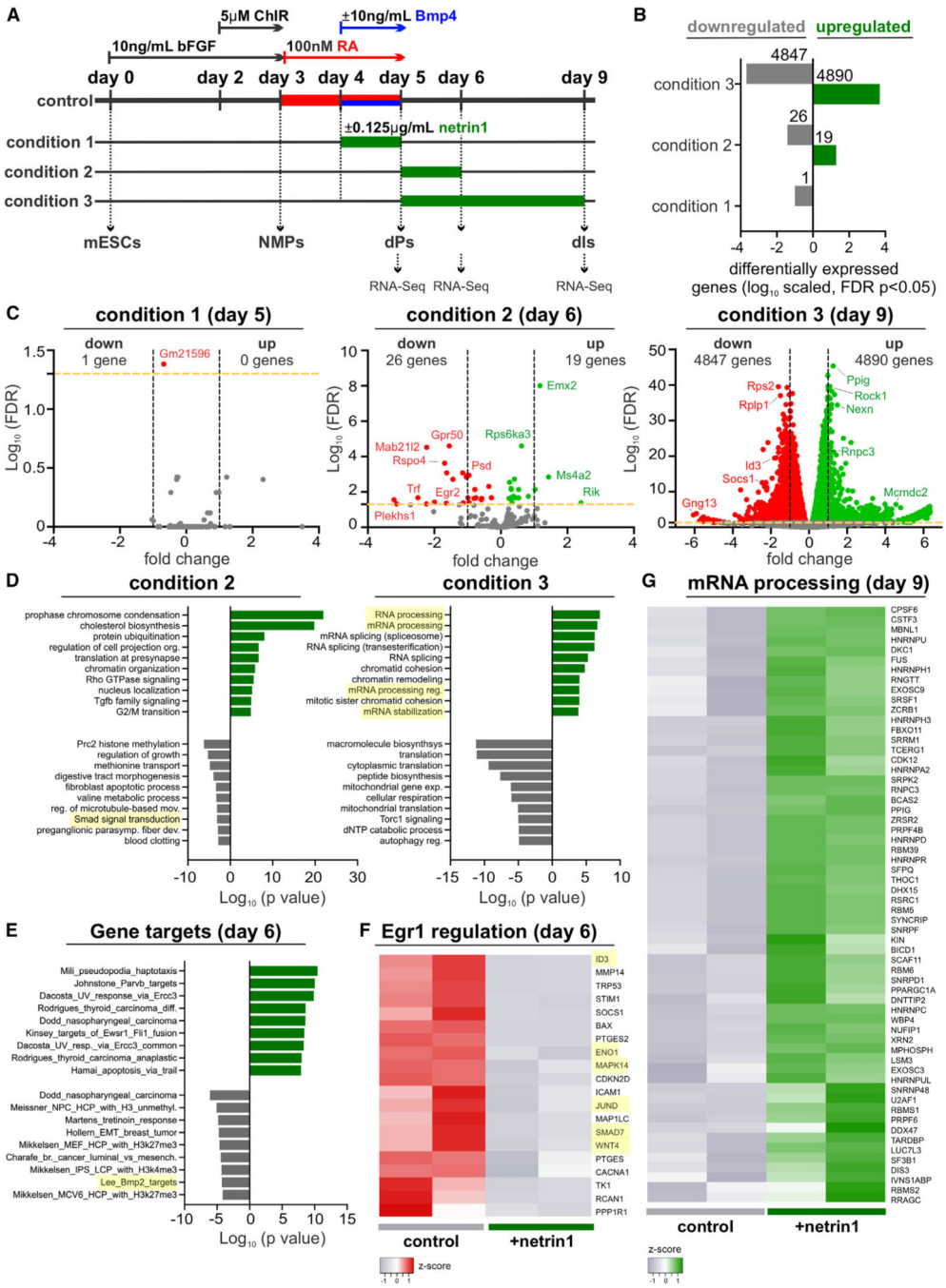


**Figure 5. Netrin1 downregulates Bmp signaling and alters mRNA processing**

(A) Netrin1 was added to the RA ± Bmp4 directed differentiation protocol at three different time points. RNA samples for bulk RNA-seq were collected on day 5 (condition 1), day 6 (condition 2), and day 9 (condition 3).

(B and C) The pulse of netrin1 in condition 1 resulted in essentially no differentially expressed genes at a false discovery rate (FDR) of $p < 0.05$. In contrast, there was a modest increase in transcriptional changes in condition 2, while ~10,000 genes were differentially

expressed in condition 3 after extended treatment with netrin1. In each case, the control condition for the differential analysis is the RA + Bmp4 condition at the same time point.
(D) GO analyses of the differentially expressed genes after netrin1 treatment showed that Bmp signaling was downregulated at day 6 and mRNA processing was upregulated at day 9.
(E) A gene target analysis of published gene sets also identifies that Bmp2 target genes (highlighted) are downregulated after netrin1 addition by day 6.
(F) Several transcription factor regulatory networks (for complete set of networks, see Table S1) were identified as being downregulated in netrin1-treated cultures in condition 3. Many Bmp target genes were found to be downregulated by Egr1 (highlighted), including Id3. The heatmap shows the Fragments per kilobase of transcript per million mapped reads (FPKM) values of select genes.
(G) Heatmap showing the upregulated expression (FPKM values) of mRNA processing genes in netrin1-treated cultures at day 9 (condition 3), validating the GO analysis in (D).

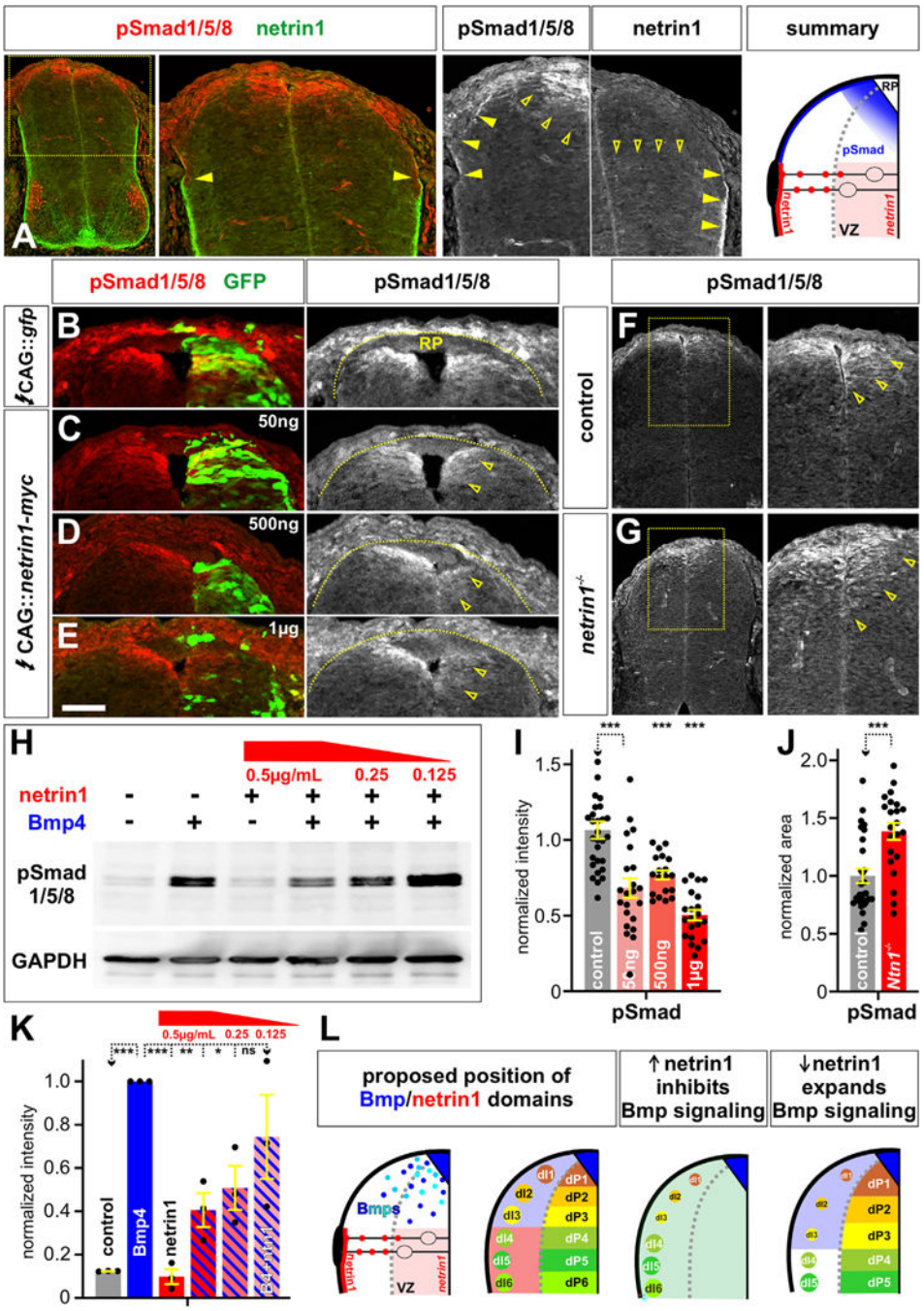


**Figure 6. Netrin1 modulates the level of Bmp signaling both *in vivo* and *in vitro***

(A) Thoracic sections of E11.5 mouse spinal cord labeled with antibodies against pSmad1/5/8 (red) and netrin1 (green). pSmad1/5/8 and netrin1 proteins are detected in neighboring domains. pSmad1/5/8 is present in the VZ immediately flanking the RP (open arrowheads) and along the pial surface of the dorsal-most spinal cord (closed arrowheads). Netrin1 is present in the intermediate spinal cord, at low levels in the VZ (open arrowheads) where *netrin1* is expressed, and high levels on the pial surface (closed arrowheads) after trafficking along the radial processes.[29]

(B–E and I) Chicken spinal cords were electroporated at HH stage 14 with *Gfp* (B) or different concentrations of *netrin1* (50 ng, 500 ng, and 1 μg) (C–E) under the control of the CAG enhancer and incubated until HH stage 24/25. Thoracic transverse sections were labeled with antibodies against pSmad1/5/8 (red). Ectopic netrin1 in the dorsal-most spinal cord resulted a ~30%–50% decrease in the levels of Smad1/5/8 compared to a control GFP electroporation.

(F, G, and J) Thoracic transverse spinal cord sections from either control (F) or *netrin1*$^{-/-}$ (G) E11.5 mouse spinal cords were labeled with antibodies against pSmad1/5/8. The loss of netrin1 resulted in a ~40% larger Smad$^{+}$ area (J), suggesting Bmp signaling had been increased.

(H and K) The interaction between netrin1 and Bmp4 was further assessed in a western analysis, using GAPDH levels as a loading control. Treating Cos7 cells with Bmp4 resulted in the robust activation of pSmad1/5/8, while treatment with netrin1 alone had no effect on Smad activation above control levels. However, if netrin1 is added together with Bmp4, there is a decrease in Smad activation in a dose-dependent manner. The highest level of netrin1 (0.5 ng/mL) resulted in a ~60% decrease in the level of pSmad1/5/8, suggesting that Bmp signaling had been suppressed.

(L) Model for the biological significance of the netrin1/Bmp interaction. Multiple Bmps are secreted from the RP where they pattern the surrounding tissue into the dorsal progenitor domains (dP1–dP3). Netrin1 acts as a boundary, coincident with the dorsal root entry zone (DREZ), to limit Bmp signaling spreading into the intermediate spinal cord. Supporting this model, the dorsal-most dIs (dI1–dI3) are preferentially lost when netrin1 is expressed dorsally. In contrast, dP1–dP3 domains expand in the absence of netrin1. Probability of similarity between control and experimental groups: *$p < 0.05$, **$p < 0.005$, ***$p < 0.0005$; Student's t test. Scale bar (A–D), 50 μm.

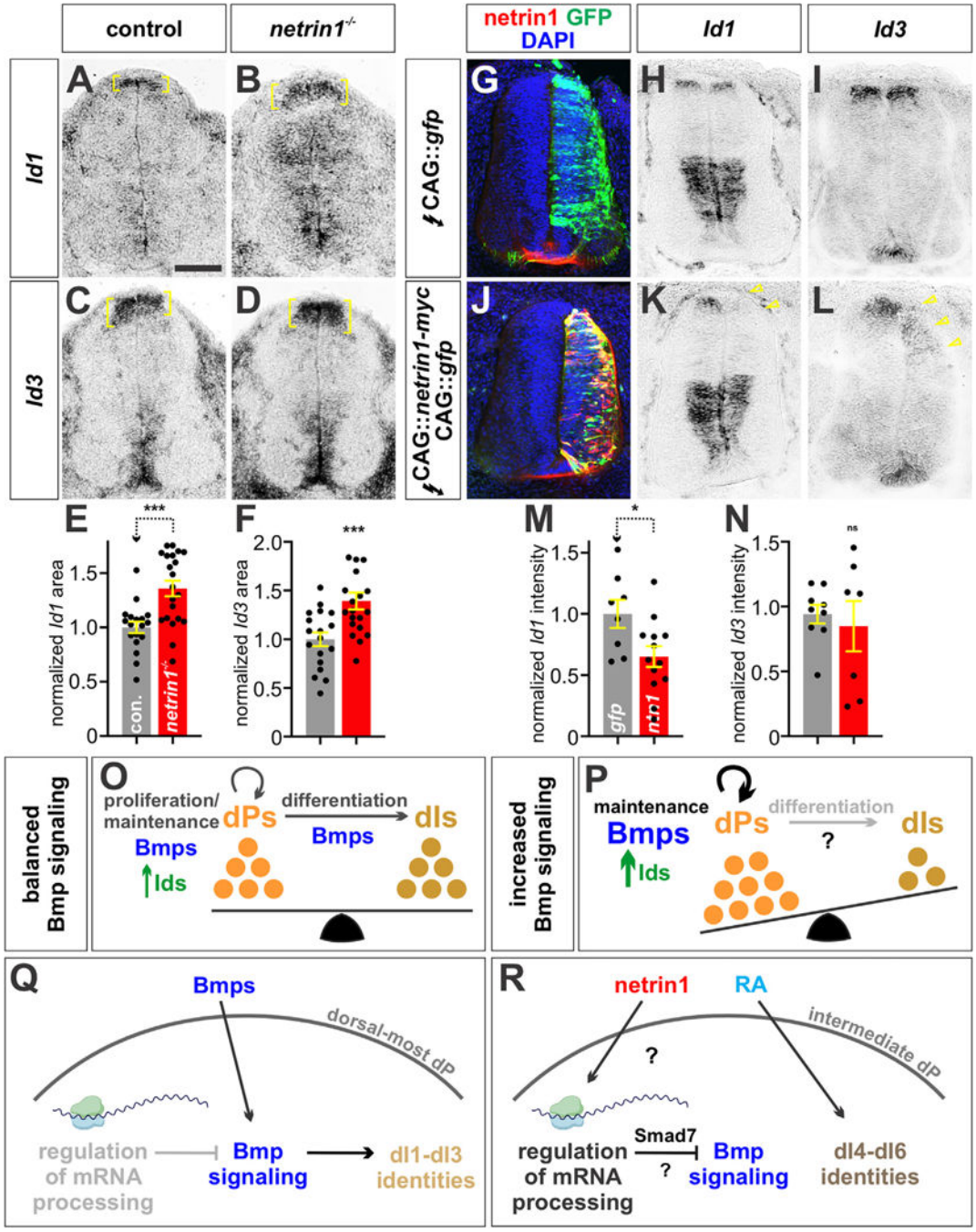


**Figure 7. *Ids* expression is increased after the loss of *netrin1***

(A–D) Control (A and C) or *netrin1*$^{-/-}$ (B and D) E11.5 mouse spinal cords were assessed for *Id1* (A and B) and *Id3* (C and D) expression in the dorsal-most spinal cord (brackets). (E and F) There is a ~35% increase in the domain of *Id1* expression (E) and a ~40% increase in *Id3* expression (F) in the *netrin1*$^{-/-}$ dorsal-most spinal cord compared to control littermates, consistent with increased Bmp signaling ($n$ = 20 sections from four embryos). (G–L) Chicken spinal cords were electroporated at HH stage 14 with *Gfp* (G–I) or 1 μg of *netrin1* (J–L) under the control of the CAG enhancer and incubated until HH stage 24.

(M and N) The electroporation of GFP had no significant effect on the intensity of *Id1* ($p > 0.12$, eight sections from four embryos) or *Id3* ($p > 0.262$, nine sections from four embryos) compared to the non-electroporated side. In contrast, there is a ~35% decrease in the level of *Id1* expression (M) when netrin1 is electroporated ($p < 0.023$, $n = 13$ sections from eight embryos). There is no significant decrease for *Id3* expression (N, $p > 0.3$, $n = 7$ sections from five embryos), although expression might be more diffuse.

(O and P) Bmps have sequential roles in the specification of dIs, directing dP proliferation, and then the differentiation of dPs into dIs[18] (O). In the absence of netrin1, we observe increased Bmp and Id signaling and an increased number of dPs, but fewer dIs (P). Since Ids are a known target of Bmp signaling, these data suggest that elevating Bmp signaling directly increases Id activity, which then maintains progenitors in an undifferentiated state and suppresses the transition to dIs.

(Q and R) In the dorsal-most spinal cord, Bmps act from the RP to activate Bmpr signaling in NPCs, thereby resulting in the activation of Ids, and other factors, needed for dP identity (Q). In the intermediate spinal cord, the presence of netrin1 acts to limit Bmp signaling, potentially through the regulation of mRNA processing, thereby permitting intermediate dP identity (R). Probability of similarity between control and experimental groups: $*p < 0.05$, $***p < 0.0005$, Student's t test. Scale bar: 100 μm.

## KEY RESOURCES TABLE

| REAGENT or RESOURCE | SOURCE | IDENTIFIER |
|---|---|---|
| Antibodies | | |
| Rabbit anti neurofilament | Cell Signaling Technology | Cat#C28E10; RRID: AB_10828120 |
| Mouse anti tubulin β3 (Tubb3)/Tuj1 | BioLegend | Cat#801202; RRID:AB_10063408 |
| Rabbit anti laminin | Abcam | Cat#11575; RRID: AB_298179 |
| Mouse anti chicken transitin/nestin | Developmental Studies Hybridoma bank | Cat#EAP3; RRID: AB_2282449 |
| Mouse anti myc tag | Abcam | Cat#ab32; RRID: AB_303599 |
| Mouse anti GFP | Invitrogen | Cat#A-11120 |
| Goat anti mouse netrin1 | R&D Systems | Cat#AF1109; RRID: AB_2298775 |
| Goat anti chicken netrin1 | R&D Systems | Cat#AF128; RRID:AB_354716 |
| Goat anti chicken netrin2 | R&D Systems | Cat#AF127; RR1D: AB_2154709 |
| Goat anti Sox2 | Santa Cruz Biotechnology | Cat# sc-17320; RRID:AB_2286684 |
| Mouse anti P27 | BD Biosciences | Cat#610241; RRID:AB_397636 |
| Rabbit anti cleaved caspase 3 | BD Biosciences | Cat#559565; RRID:AB_397274 |
| Rabbit anti phospho histone H3 | Cell signaling Technology | Cat#9701; RRID:AB_33153 |
| Goat anti Lhx2 | Santa Cruz Biotechnology | Cat#Sc-19344; RRID:AB_2135660 |
| Rabbit anti Lhx2 | Gift from Tom Jessell; Liem et al.[13] | N/A |
| Mouse anti Lhx1/5 | Developmental Studies Hybridoma bank | Cat#4F2; RRID:AB_531784 |
| Guinea Pig anti Tlx3 | Gift from Thomas Muller; Muller et al.[76] | N/A |
| Mouse anti Isl1/2 | Developmental Studies Hybridoma bank | Cat#39.4DS |
| Goat anti Isl1/2 | R&D Systems | Cat#AF1837, RRID:AB_2126324 |
| Rabbit anti Pax2 | Invitrogen | Cat#71-6000 |
| Guinea Pig anti Olig2 | Gift from Bennett Novitch; Novitch et al.[62] | N/A |
| Rabbit anti Math1/Atoh1 | Helms and Johnson[77] | N/A |
| Goat anti Ascl1/Mash1 | R&D Systems | Cat#AF2567; RRID:AB_2059505 |

| REAGENT or RESOURCE | SOURCE | IDENTIFIER |
|---|---|---|
| Guinea Pig anti Foxd3 sera | Gift from Thomas Muller; Muller et al.[76] | N/A |
| Rabbit anti Gapdh | Protientech | Cat# 10494-1-AP; RRID:AB_2263076 |
| Rabbit anti Phospho-Smad1 (Ser463/465)/Smad5 (Ser463/465)/Smad8 (Ser465/467) (D5B10) | Cell Signaling Technology | Cat#11971; RRID:AB_2797785 |
| Chemicals, peptides, and recombinant proteins | | |
| Mouse Recombinant netrin1 | R&D | Ca#1109-N1-025 |
| Human Recombinant Bmp4 | Thermo Fisher Scientific | Cat#PHC9534 |
| Retinoic acid | Sigma Aldrich | Cat#R2625 |
| Human basic FGF (bFGF) | Thermo Fisher Scientific | Cat#PHG0023 |
| Neurobasal medium | Thermo Fisher Scientific | Cat#21103049 |
| B27 supplement | Fisher Scientific | Cat#17-504-044 |
| N2 supplement | Thermo Fisher Scientific | Cat#17502048 |
| CHIR99021 | Tocris | Cat#4423 |
| Paraformaldehyde 16% | Sigma-Aldrich | Cat#28906 |
| Prolong Gold | Thermo Fisher Scientific | Cat#P36930 |
| Blotting-Grade Blocker | Bio Rad | Cat#1706404 |
| cOmplete™, EDTA-free Protease Inhibitor Cocktail | Roche | Cat#04693132001 |
| PhosSTOP™, Phosphatase Inhibitor | Roche | Cat#4906845001 |
| 30% Acrylamide/Bis Solution, 37.5:1 | Bio Rad | Cat#1610158 |
| 10x Tris/Glycine/SDS | Bio Rad | Cat#1610732 |
| Critical commercial assays | | |
| SuperSignal™ West Femto Maximum Sensitivity Substrate | Thermo Scientific | Cat#34094 |
| RNeasy plus mini kit | Qiagen | Cat#74106 |
| DIG RNA Labeling Kit | Roche, Millipore | Cat#11175025910 |
| Superscript IV First-Strand synthesis kit | Thermo Fisher Scientific | Cat#18091050 |
| Deposited data | | |
| Bulk RNA-Seq | Gene Expression Omnibus (GEO) repository | GEO: GSE246903 |
| Experimental models: Cell lines | | |
| Cos7 cells | ATTC | ATCC CRL-1651 |
| MM13 mouse embryonic stem cell line | Gift from Tom Jessell, Columbia University Wichterle et al.[54] | N/A |

| REAGENT or RESOURCE | SOURCE | IDENTIFIER |
|---|---|---|
| Experimental models: Organisms/strains | | |
| Mouse: Netrin1 null line | Lisa Goodrich Lab, Harvard University Yung et al.[60] | N/A |
| Chicken: Fertile Leghorn chicken eggs | CJ Eggs, Sylmar, Ca | N/A |
| Oligonucleotides | | |
| Forward *in situ* probe for chicken *netrin1*: 5′-GACATCCACATCCTGAAAGCGGA-3′ | this paper | N/A |
| Reverse *in situ* reverse probe for chicken *netrin1*with T7 sequence attached: 5′-GACTAATACGACTCACTATAGGGTTTCCCCTTCCATCCCTCAA-3′ | this paper | N/A |
| Forward *in situ* probe for chicken *netrin2*: 5′- GACTTTCTTGTGCAGCAGAGACG-3′ | this paper | N/A |
| Reverse *in situ* probe for chicken *netrin2* with T3 sequence attached: 5′-GACATTAACCCTCACTAAAGGGACTCTCC TCTCTTCCTGCCAC | this paper | N/A |
| Forward *in situ* probe for mouse *Id1*: 5′- TCAGGAGGCAAGAAGAAAAA-3′ | this paper | N/A |
| Reverse *in situ* probe for mouse *Id1* with T3 sequence attached: 5′-GAGATTAACCCTCACTAAAGGGAAGAAATCCGAGAAGCACGAA-3′ | this paper | N/A |
| Forward *in situ* probe for mouse *Id3*: 5′- GACTCTGGGACCCTCTCTCC-3′ | this paper | N/A |
| Reverse *in situ* probe for mouse *Id3* with T3 sequence attached: 5′-GAGATTAACCCTCACTAAAGGGATAATCAGGGCAGCAGAGCTT- 3′ | this paper | N/A |
| Forward qPCR primer for *Lhx2*: 5′- CAGCTTGCGCAAAAGACC-3′ | this paper | N/A |
| Reverse qPCR primer for *Lhx2*: 5′- TAAAAGGTTGCGCCTGAACT-3′ | this paper | N/A |
| Forward qPCR primer for *Lhx9*: 5′- CAGGCCTGACCAAAAGAGTT-3′ | this paper | N/A |
| Reverse qPCR primer for *Lhx9*: 5′- TGCCGTCAGCTTTATCAACA-3′ | this paper | N/A |
| Forward qPCR primer for *Foxd3*: 5′- CCCCAACACTGACCAACAG-3′ | this paper | N/A |
| Reverse qPCR primer for *Foxd3*: 5′- GTTTGCTCCGCCAGCTTA-3′ | this paper | N/A |
| Forward qPCR primer for *Isl1*: 5′- AGGACAAGAAACGCAGCATC-3′ | this paper | N/A |
| Reverse qPCR primer for *Isl1*: 5′- TTCCTGTCATCCCCTGGATA-3′ | this paper | N/A |
| Forward qPCR primer for *Gapdh*: 5′- GGCCTTCCGTGTTCCTAC-3′ | this paper | N/A |
| Reverse qPCR primer for *Gapdh*: 5′- TGTCATCATACTTGGCAGGTT-3′ | this paper | N/A |
| Recombinant DNA | | |
| mouseNtn1-AP-His | Addgene | RRID:Addgene_71978 |
| pCMV-GFP | Addgene | RRID:Addgene_11153 |
| pCAG::*Ntn1-c-myc* | this paper | N/A |
| Software and algorithms | | |
| Zen Blue Lite | Zeiss | https://www.zeiss.com/microscopy/us/products/microscope-software/zen-lite.html |
| Zen Black | Zeiss | https://www.zeiss.com/microscopy/us/products/microscope-software/zen-lite.html |
| Azure Western Blot Imaging Software | Azure Biosystems | https://azurebiosystems.com/ |

| REAGENT or RESOURCE | SOURCE | IDENTIFIER |
|---|---|---|
| ImageJ | National Institutes of Health | https://imagej.nih.gov/ij/ |
| Prism 9 | Graphpad | https://www.graphpad.com/scientific-software/prism/ |
| Corel DRAW version 24 | Corel DRAW | http://www.coreldraw.com |